EXCURSION GUIDE

IAG REGIONAL CONFERENCE 2011

GEOMORPHOLOGY FOR HUMAN ADAPTATION TO CHANGING TROPICAL ENVIRONMENTS

ADDIS ABABA, ETHIOPIA FEBRUARY 18-22, 2011

ORGANIZED BY

EAG - ETHIOPIAN ASSOCIATION OF GEOMORPHOLOGISTS

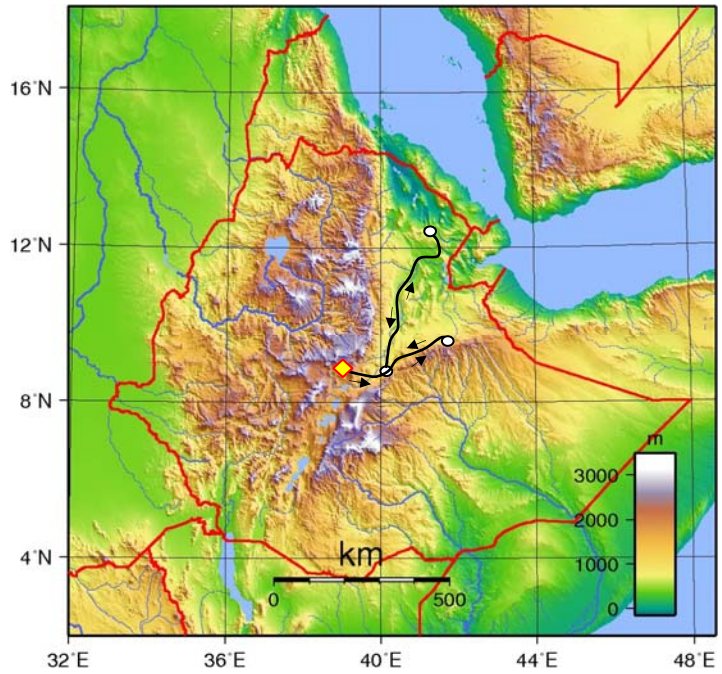

Pre-conference excursion

Tectonic Landforms and Volcanism in the Southern Afar

13 – 18 February 2011

Acocella Valerio, Bekele Abebe, Coltorti Mauro
(Eds.)

1 – General geology of the Afar area

In Central Afar, the Red Sea and Aden propagators meet with the northern portion of the Main Ethiopian Rift (MER), deforming a broad area and developing microplates (Danakil microplate; McKenzie et al., 1970; Le Pichon and Francheteau, 1978). The mean spreading rates of the Aden propagator and the northern portion of the Red Sea propagator are ~1.1 cm/yr and ~2 cm/yr respectively, significantly higher than the ~2.5 mm/yr of MER. This suggests that most of the strain in Afar results from the activity and interaction of the Aden and Red Sea propagators (Tapponnier et al., 1990).

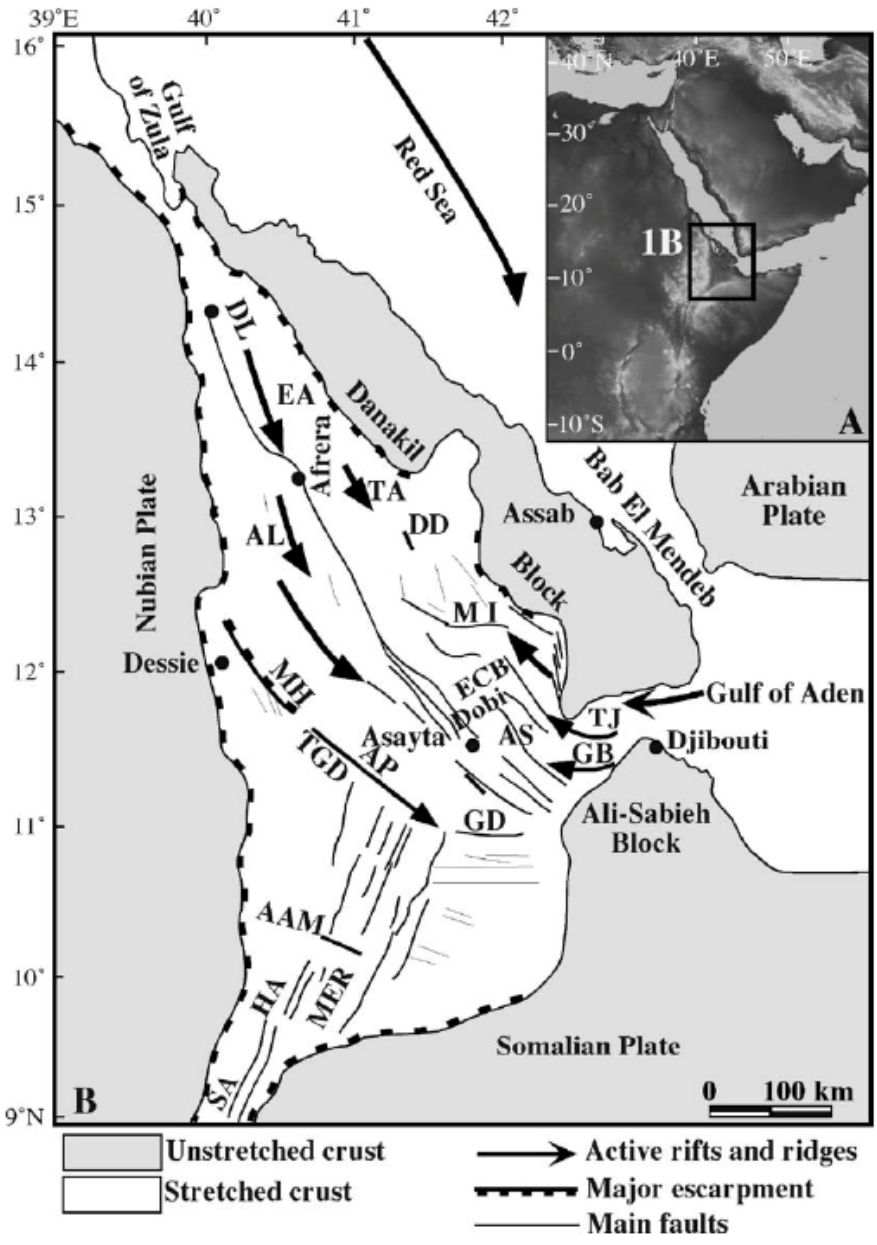

The Afar region

Volcanic activity has accompanied the development of the triple junction; its evolution can be summarized through 3 main stages: a) the emplacement of the widespread and thick “Stratoid” sequence (Kidane et al., 2003, and references therein), made up of flood basalts and ignimbrites, marking the transition to an oceanic crust, from 4 to 1 Ma; b) the development of central silicic volcanoes, as precursors to rift propagation, in the last 2 Ma; c) the current oceanic-type basaltic volcanism, along the active rift zones (Barberi et al., 1972; Barberi et al., 1975; Beyene and Abdelsalam, 2005, and references therein).

The Aden propagator mainly consists of two NW-SE trending rift segments: these are the Asal-Ghoubbet Rift, to the south, and the Manda Inakir Rift, to the north. The two segments are connected by an oblique transfer zone, characterized by the rotation about a vertical axis of small rigid blocks (Manighetti et al., 2001; and references therein). Each segment essentially consists of subvertical to riftward-dipping active normal faults and an axial portion of active tensile fracturing and volcanic activity.

The less studied Red Sea propagator is characterized, to the north, by the Erta Ale Range, which separates the Ethiopian Plateau from the Danakil Block. The Erta Ale Range consists of a NW-SE alignment of active volcanoes, largely shield volcanoes with basaltic composition, associated with fracturing (Barberi and Varet, 1977). To the South, the Red Sea propagator branches into an eastern segment, the Tat'Ali Rift, and a western segment, which propagates into Central Afar and we named southern Red Sea propagator. This includes the NW-SE trending Tendaho Graben (TG), the largest basin of Central Afar and the active NW-SE trending Manda Hararo Rift (MHR; Tapponnier et al., 1990; Manighetti et al., 2001; Acocella et al., 2008). TG marks the northern limit of the MER structures. TG, formed in the last ~1.8 Ma (Acton et al., 2000), is several tens of km wide and a few hundred kilometres long and hosts eruptive fissures and central volcanoes. Its bedrock mainly comprises Stratoid deposits, which generally young towards the central part of the graben (Lahitte et al., 2003; Kidane et al., 2003). The infill of TG, overlying the Stratoids, consists of volcanic and sedimentary deposits, among which are, to the NW, the youngest basaltic deposits (0.22-0.03 Ma; Lahitte et al., 2001) of the axial part of MHR. The northernmost part of MHR, in the Dabbahu area, underwent a major rifting episode in 2005, associated with the emplacement of a dike 60 km long and up to 8 m wide. Dike intrusion was accompanied by seismic activity. The 2005 episode shows the importance of catastrophic magma emplacement in the development of the rift (Wright et al., 2006; Hamling et al., 2010). To the south, MHR grades into the northern TG (Fig. 1b).

MER reached Afar propagating northwards in the last 11 Ma. NNE-SSW trending MER is characterized by a progressive widening northwards, decreasing the length of its rift segments, the separation of the magmatic centres and the effective elastic thickness of the crust (Ebinger and Hayward, 1996; Hayward and Ebinger, 1996, Ebinger and Casey, 2001).

2 – SOUTH WESTERN SIDE OF AFAR

Excursion stop sites: Bekele Abebe and Valerio Acocella

1st day. February 13th

Stop 1: Gariboldi Pass

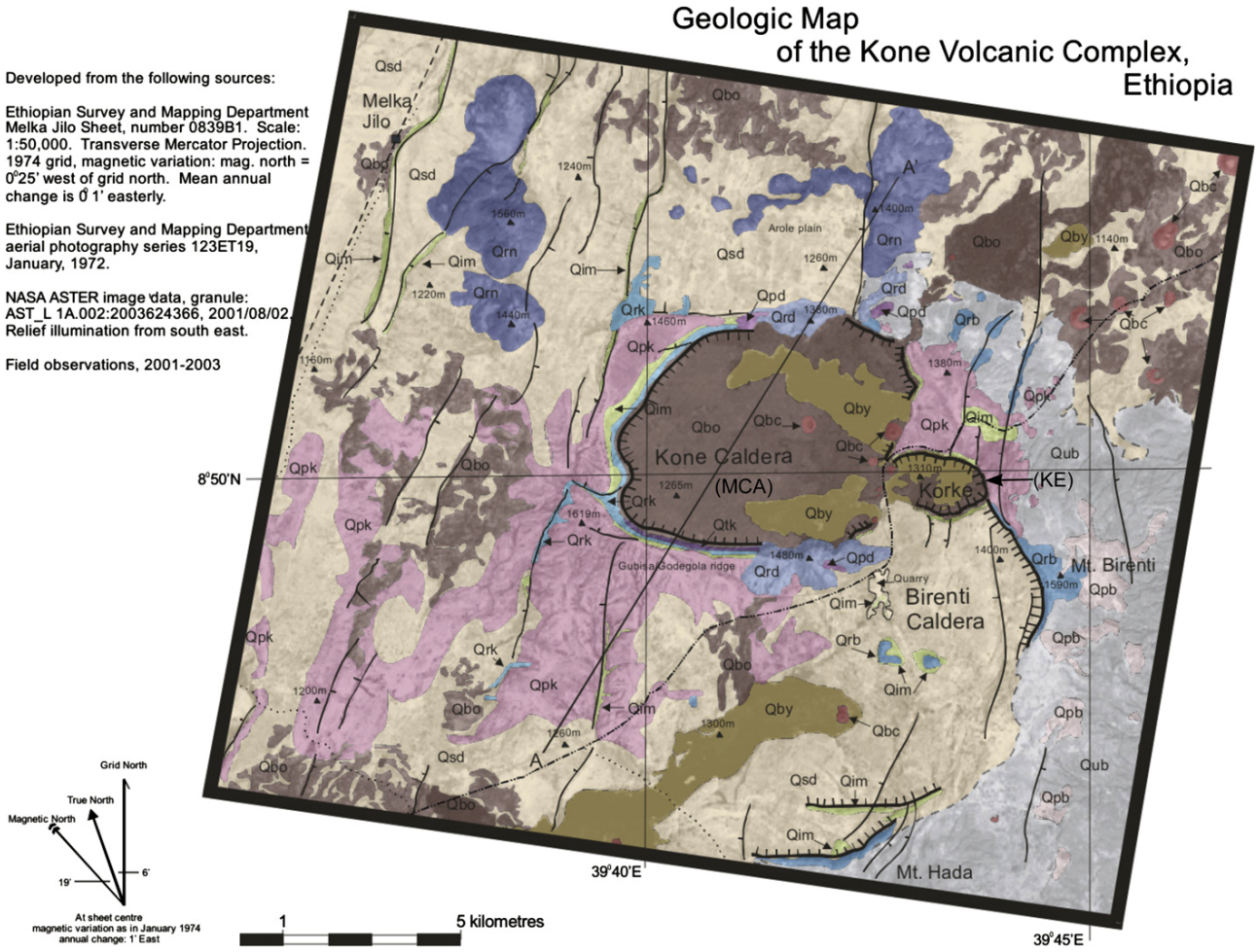

Fig. 1 – Gariboldi Volcanic Complex (Rampey et al., 2010)

Gariboldi Volcanic Complex

Gariboldi (or Kone) Volcanic Complex is characterized by seven nested calderas, ranging from Pleistocene to Recent (Fig. 1; Mohr, 1962; Cole, 1969; Rampey et al., 2010).

The largest and most recent caldera is associated with pumice and ash fallouts. Two smaller calderas in the eastern side of the complex are associated with ignimbrites and rhyolitic lava flows. The rock types identified at Gariboldi are mainly trachytes, rhyolitic lavas associated with ignimbrites, pumice and few recent basaltic flows. Cole (1969) has identified three silicic phases and one mafic phase in the volcanic history of the area.

This stop at the Gariboldi Pass permits to observe the two most recent E-W elongated calderas of the Gariboldi complex (located at the East and the West of the Pass). The largest caldera, to the west, is partly filled by recent lava flows, erupted from a NNE-SSW trending fissure, as shown by the alignment of several spatter cones.

Stop 2: MeteHara Lake

Fantale volcano

Fantale, immediately to the N of Gariboldi, is one of the most active volcanoes on the Ethiopian Rift. Its magmatic history has been dominated by the eruption of intermediate and silicic volcanics, characterized by a large quantity of ignimbrites, pumice and ash fallout at its early stage and lava flows (obsidian and rhyolites) at late stages (La Croix, 1930; Rohleder and Hitchen, 1930; Mohr, 1962; Gibson, 1967). Fantale last erupted obsidian flows and basaltic lavas in 1820 (Gibson, 1967) and is presently characterized by an E-W elongated caldera (Fig. 2).

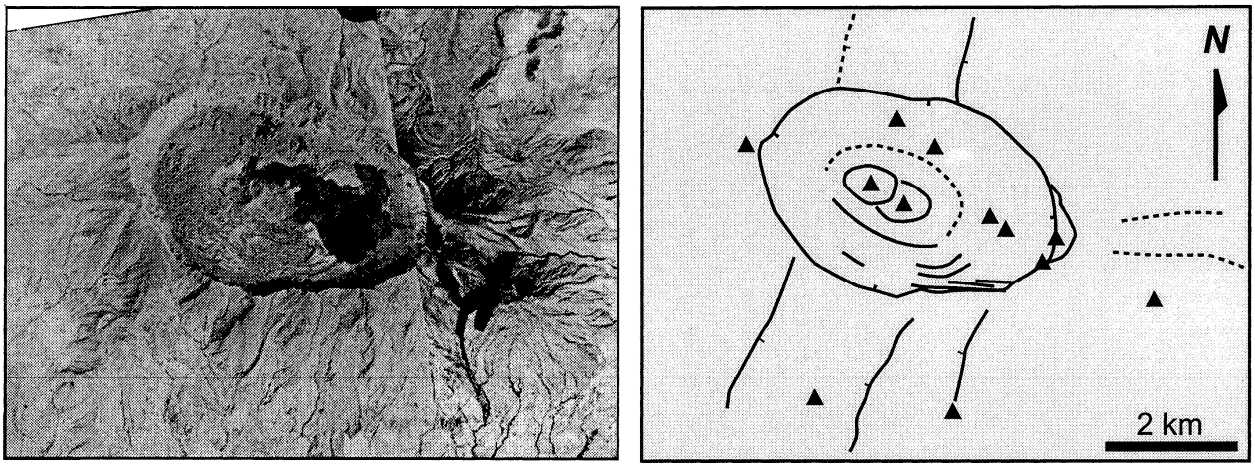

Fig. 2 – Aerial view of Fantale volcano, and related structural sketch, reporting the main features (Acocella et al., 2002)

Active normal faults within the Rift axis and their formation

This outcrop on the S slope of Fantale, next to MeteHara Lake, allows to observe a wonderfully exposed active normal fault, which is representative of the normal faults outcropping within the axis of the Rift (Fig. 3). The foot wall and the hanging wall of the faults are separated by an open area, bordered by vertical walls: the normal fault is and thus a subvertical open fault at surface, with a dilational component (Fig. 3). The layers in the hanging wall regularly show a tilt, usually between 10° and 50°, towards the downthrown side. Such a tilt is responsible for a real throw much larger (few tens of meters) than the apparent one (several meters) observed at the sides of the open area.

Fig. 3 – Open normal fault on the S slope of Fantale volcano (the volcano is on the background).

This type of open (= with a dilational component) normal fault is observed only along divergent plate boundaries, as for example also in Iceland (Gudmundsson, 1992). Two main mechanisms have been invoked to explain the formation of open normal faults.

1) These faults are inferred to form from the growth of extensional fractures, from surface to depth, within the axial part of the rift (Gudmundsson, 1992; Acocella et al., 2003). Once the extension fractures grow along their strike and dip (stage a in Fig. 4), they reach a critical depth h_c (stage b in Fig. 4), where the pure tensile stresses, because of the lithostatic load at depth, are no longer sustained. At this point, the tensile fractures turn into shear fractures, developing normal faults (stage c in Fig. 4). The change from tensile to shear modalities implies a decrease in the dip of the fault with depth; this leads to the development of the drag (tilt) observed in the hanging wall.

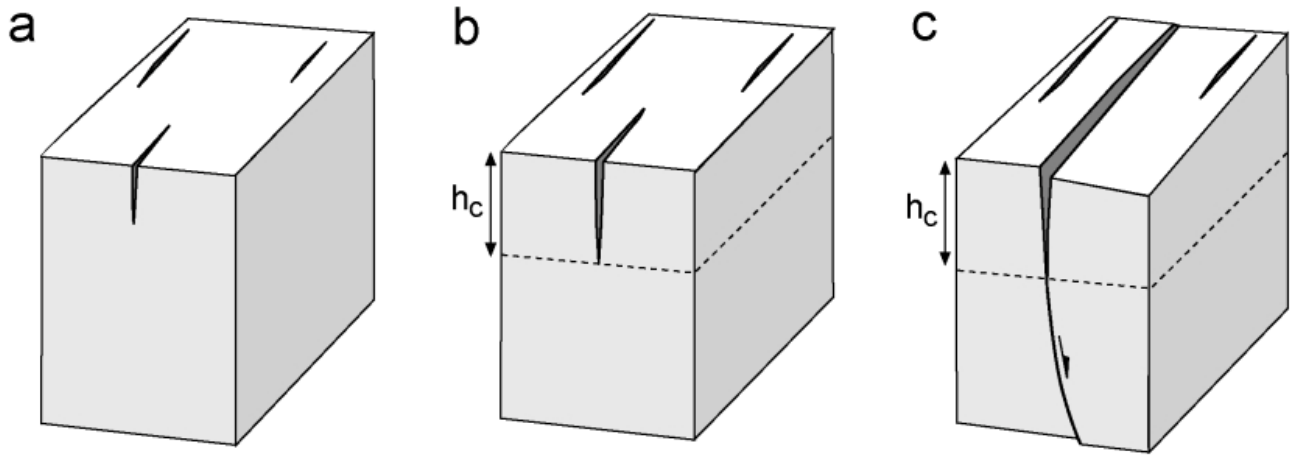

Fig. 4: A model suggested to explain the formation of open normal faults (Acocella et al., 2003)

2) The open normal faults are related to the upward propagation of a dike, which induces faulting and fracturing at its upper tip (Fig. 5: e.g. Rowland et al., 2007). The open normal fault propagates upward and the tilt in the hanging wall is interpreted to result from the elastic bending at the fault tip, later dissected by the fault itself, when reaching the surface; therefore, the tilt is the expression of a fault-propagation fold. This mechanism is based on recent evidence of dike intrusion in Central Afar (Dabbahu volcano) where it as been possible to observe that it is the magma that splits the plates apart within the rift zone, emplacing dikes responsible for faulting and fracturing at the surface (Wright et al., 2006; Sigmundsson, 2006).

At the present, there is robust evidence that both mechanism 1) and 2) are active along divergent plate boundaries, explaining the development of open normal faults.

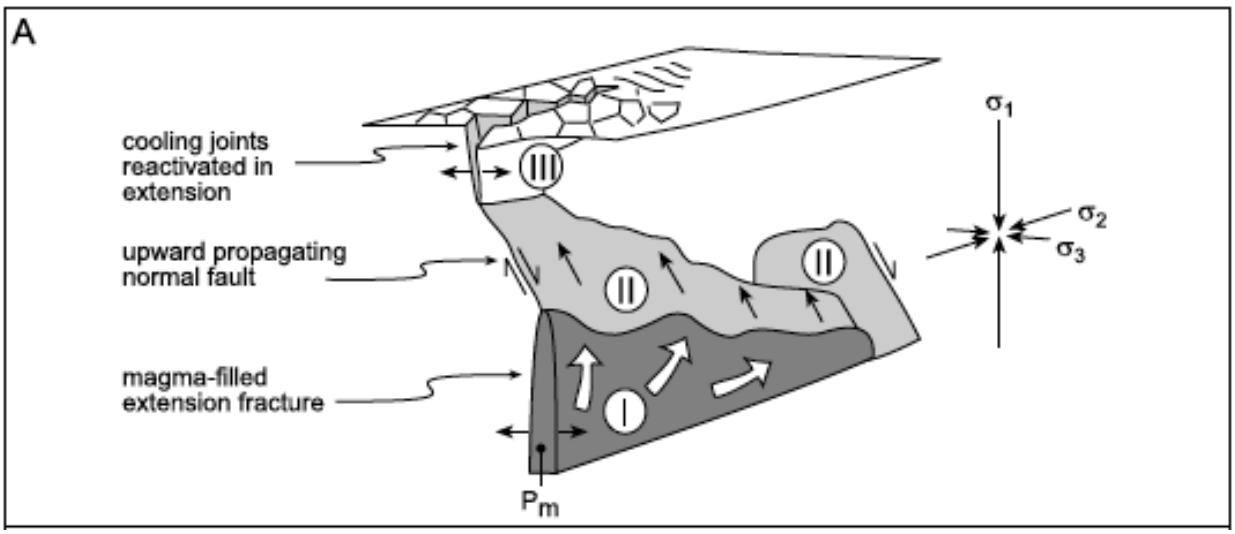

Fig. 5: An alternative mechanism to explain the development of open normal faults along divergent plate boundaries (Rowland et al., 2007).

THE SOUTHERN BORDER OF THE AFAR

3 - Excursion stop sites: Bekele Abebe and Mauro Coltorti

This part of the field trip is devoted to illustrate the geomorphology of the major fault escarpment that constitute the southern border of the Afar depression in the Dire Dawa district (Fig.6). This southern escarpment originates at the junction with the MER, near Asela, and continue eastward bordering to the south the Gulf of Aden. It is the major geomorphological feature separating the Somalian plate to the south from the Afar depression to the north. Moving from west to east inside the Afar the continental crust is progressively thinner and in the Gulf of Aden it is possible to observe the transition to the oceanic crust. The opening of the Afar depression, that occurred with the activation of E-W trending normal faults, is usually attributed to the Late Miocene. The geological sequence is similar to that evidenced in large part of "Horn of Africa" and the Arabian Peninsula although some major variations have been pointed out by Bosellini et al. (2001). These Authors recognized five major depositional sequences separated by important unconformities. From bottom to top:

1. ***Metamorphic basement***: mostly made of strongly deformed low grade metavolcanics and metasediments, upper Precambrian in age. Batholiths of Late Precambrian-Early Paleozoic age are also present.
2. ***Adigrat Sandstone*** (also known as "***Lower Sandstone***"): mainly fluvial cross bedded sandstones indicating wide alluvial plains crossed by meandering rivers. A gradual transition to fossiliferous coastal deposits has been observed close to Harar. The thickness range from 0 to ca. 100 m. The age is Late Triassic-Early Jurassic (Bosellini et al., 2001).
3. ***Antalo Supergroup*** made of**:**
    1. **Antalo Limestones:** split in two members and characterized by a thickening upward sequence. The lower part is made of fossilifeours bioturbated dark grey marls and marlstones capped by dark grey grainstones. The upper part is made of dark sandstones and grainstones. Thickness: ca. 100 m. The age is Callovian-Oxfordian.
    2. ***Dire Dawa Formation***: made of thinly bedded nodular black mudstone with thin lenses and layers of black chert. Fine grainstone beds interbedded with marly limestones are present at the top. Thickness: 10-25 m. Early Kimmeridgian in age.

3. ***Daghani Shales***: in the lower part marly limestones and marls rich in ammonites and molluscs; in the upper part shales, silstones and selenitic gypsum. Thickness: ca. 50 m. Middle-Late Kimmeridgian in age.
4. ***Gildessa Limestone***: corals in a reefal setting. Thickness: ca. 20 m. Early Titonian in age.

4. **Amba Aradom** Formation (also known as "**Upper *Sandstone***"): coastal to alluvial white quartzarenites and well rounded quartz conglomerate layers and lenses. Local shale intercalations. Thickness: 50 to 150 m. Early Aptian in age.
5. **Continental Flood Basalts** (CFB), also know as Trap Vulcanics. It is made of basalts with some intercalation of rhyolites in the upper part. Thickness: ca. 300-400 m. According to the most recent dating the sequence was deposited in a short period between 30.5 and 21 Ma (Chernet et al., 1998; Coulié et al., 2004). Their emplacement occurred mostly along fissures and small neck. At depth batholites, laccoliths and sills were also emplaced and their number and size increase moving northward inside the Afar. Their deposition generated a large volcanic plateau.
6. **Afar Flood Basalt** (AFB): porfiric, tholeitic and comenditic basalts with local intercalations of siliceous lavas in the upper part. They are found in the Afar depression floor. In the study area thickness is between 20 and 100 m. Age is debated and ranges between 4 Ma and less than 1 Ma. Ages of 0.63 Ma have been obtained very close to the study area by Audin et al., (2004).

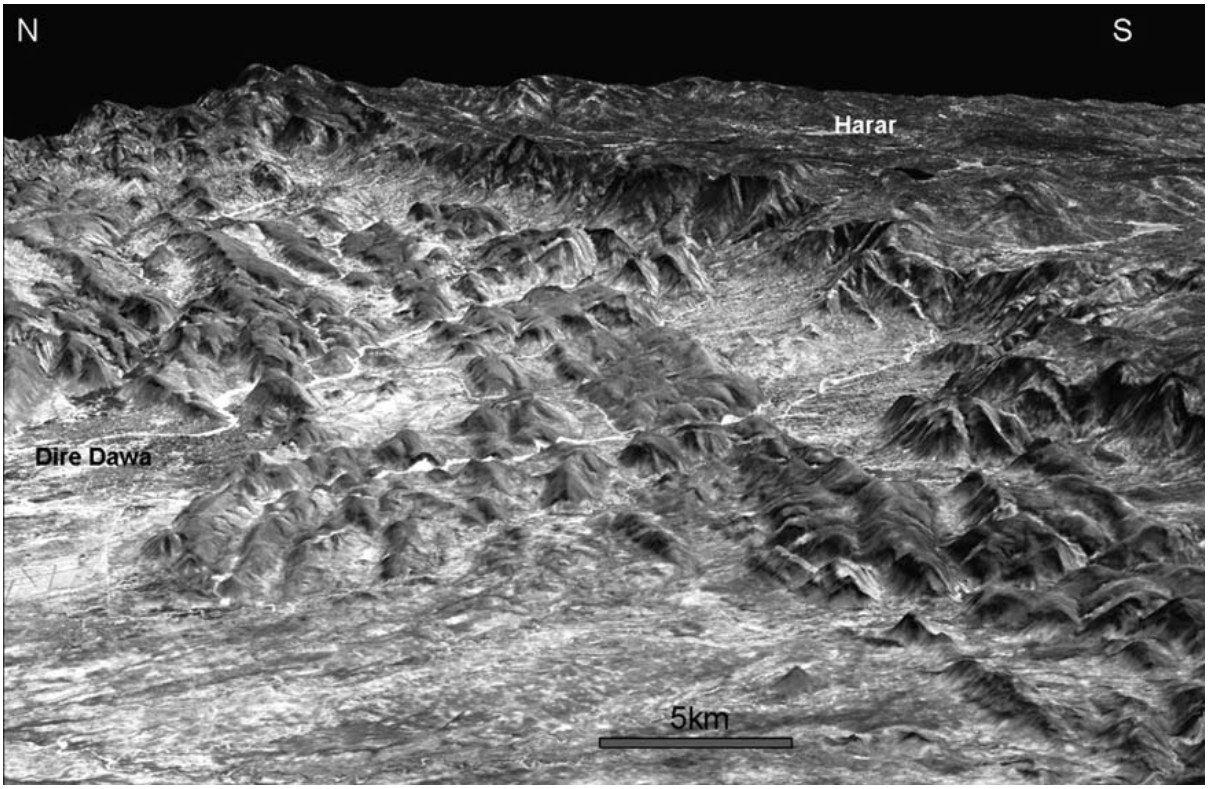

Fig. 6 – Aster image (3n21) draped on the SRTM DEM showing the structural setting of the Somali Plateau escarpment made up by faulted blocks tilted toward the south

Although re-exumation of the unconformities separating the different successions played a major role in the modelling of landscape in other parts of Ethiopia (Coltorti, 2007) this occurred only to a minor extent in the study area. Selective erosion generated stepped slopes that are easily recognizable out of the fault escarpments. The major landscape inherited from the geological history and still playing a major role in the reconstruction of the geomorphological evolution of the area is the **volcanic plateau**. The Gara Muleta Amba (amba is the Ethiopian term used for the mesas), reaches an elevation of almost 3.600 m and constitutes the top depositional surface of the CFB. Another isolated relief capped by CFB crop out to the east of Harar, in the Jijiga area (Pizzi et al., 2008). These remains represent the starting point of all the successive changes in the landscape because they were deposited, during the Oligocene, over a flat topography, possibly not far from the sea level. In fact the pre-CFB unconformity surface, modelled on coastal deposits, is almost tabular and no major incisions have been described separating the deposition of the basalts. This is a pre-Rift morphology preserved not only on the relief along the edges of the Afar depression but also in Yemen and other parts of the Arabian Peninsula.

Moving westward the scattered remnants enlarge progressively and generate a well preserved volcanic plateau. The mean elevation, around 3.500 m, can be roughly used to evaluate the amount of uplift since the Oligocene. However, we cannot exclude that the area remained stable and underwent to an acceleration of uplift only during the rifting processes, to which uplift is most likely associated.

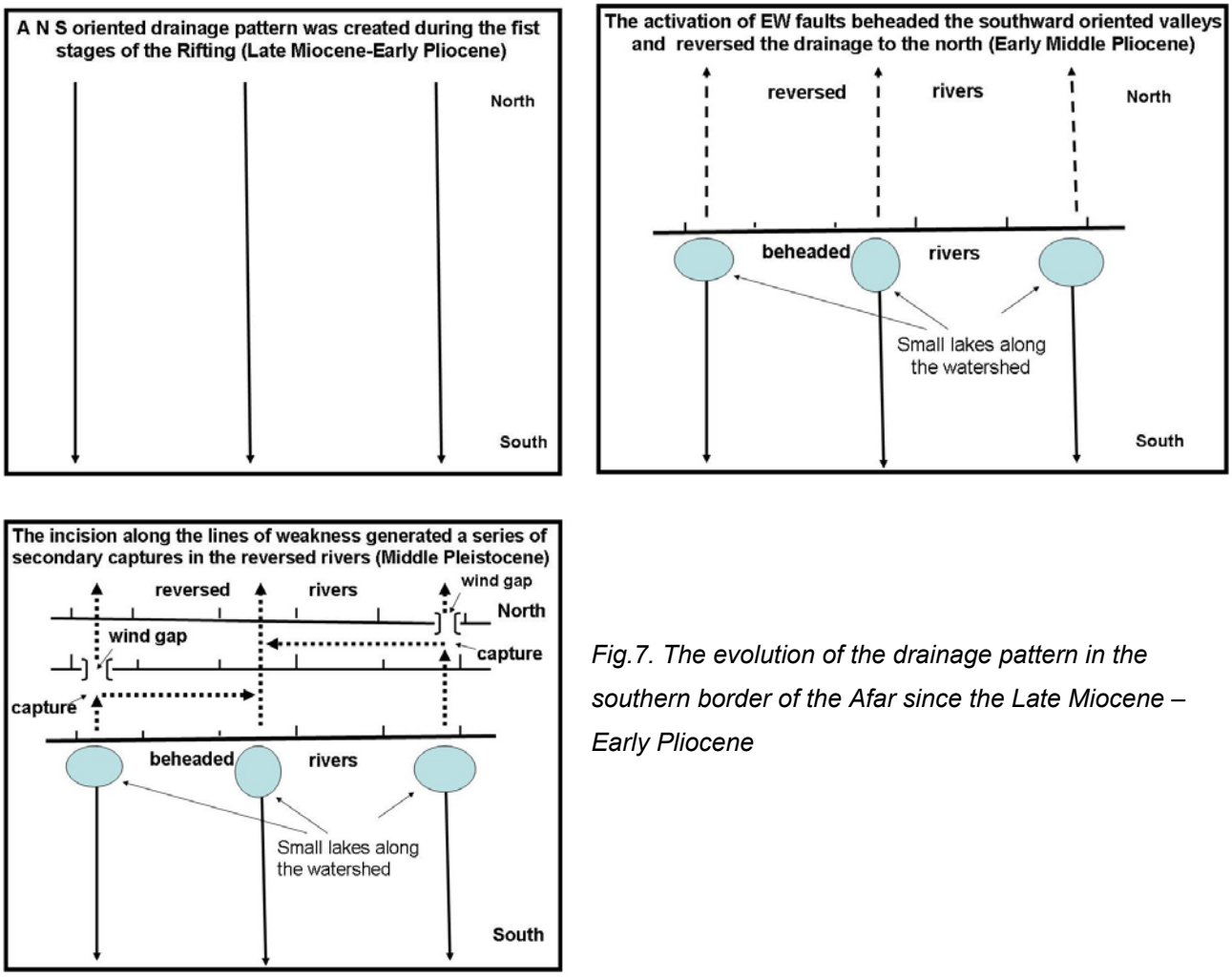

Fig.7. The evolution of the drainage pattern in the southern border of the Afar since the Late Miocene – Early Pliocene

The analysis of the drainage pattern (Fig.7) allow us to establish which were the earliest flow directions and the changes that occurred as a response of fault activation during the rift process. A series of wind gaps, that represent the remains of the pre-rift drainage, characterize the watershed above the main escarpment. They are locally associated with small lakes which constitute the source area of south oriented rivers. The difference in elevation from the top of the volcanic plateau (3.550 m) to the wind gap in the main watershed (2.200 m) is in the order of 1400 m and represent the amount of river down-cutting before the onset or during the first phases of the rifting. The former southward oriented drainage was the consequence of a general arching in the first stages

of the Rift. Later on, when the fault activity became stronger and rivers were no more able to erode the relief, the southward valleys were beheaded and the drainage was reversed northward inside the Afar depression.

The drainage pattern along the escarpment was conditioned the presence of a series of faults and faulted blocks. The faults are mostly oriented E-W but locally there are segments turning progressively to the NW and to a minor extent to the NE, delimiting large blocks. NNE trending lineaments have also been recognized and correspond to older faults and fractures affecting the basement rocks (Ghebraeb, 1998) frequently intruded by dolerites. The E-W faults are closely spaced, usually delimiting blocks 1 to 2 km wide. The total width of the escarpment is between 20 and 30 km giving a rough idea of the number of faults in this sector. The major normal faults are high angle, dipping 80-60°, and displacements can reach 1000m. The bedrock successions above the escarpment are almost horizontally layered but moving inside the faulted blocks they are tilted up to 60°. The kinematic indicators measured along the fault planes shows a slightly left oblique component suggesting a s3 (sigma) axe of the paleostress oriented NNW-SSE. Some fault planes have two different sets of striae indicating an older direction of extension coherent with a s3 axe oriented NNE-SSW. In the Dire Dawa area we also observed couples of footwall anticline-hanging-wall syncline at the border and inside the faulted monoclines (Fig.8). This evidence have been associated with a process of fault-propagation folding in extensional regime (Morton & Black, 1975; Pizzi et al., 2008).

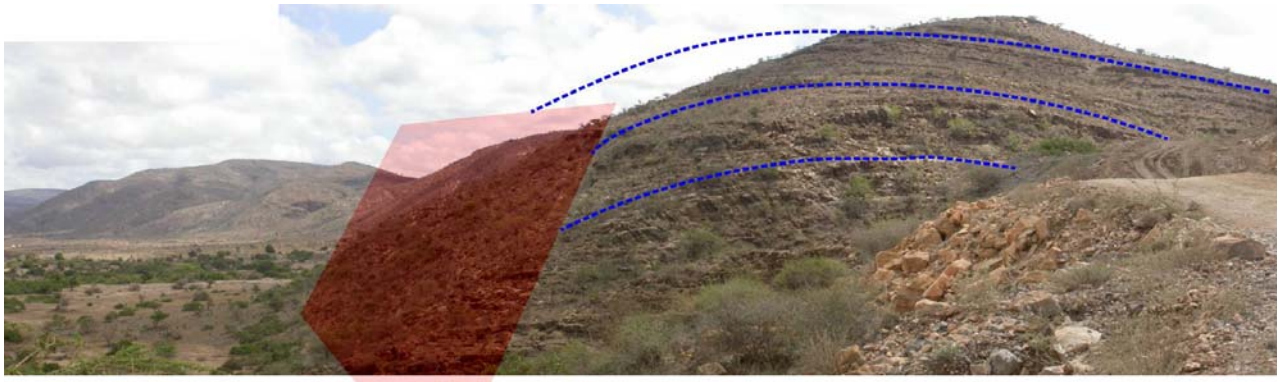

Fig. 8 Fault escarpments with evidence of the rotation affecting the sedimentary succession.

The structural style could be explained with the “domino faulting” model of Morton & Black (1975) although Pizzi et al. (2007) along the border of the Main Ethiopian Rift suggested a mixed behaviour with single faults listricating at depth inside a major weakness horizon, a detachment-like surface.

The valley incision proceeded along the different sets of faults generating an angular drainage pattern that isolated a series of blocks. The reversed main river courses were originally oriented to the N but the accelerated erosion along the lines of weakness, represented by the E-W fault planes, generated a series of elbows and wind gaps on the secondary watershed indicating a large number of river captures.

The analysis of the ridges below the main escarpment allow us to recognize a further major landscape feature (Fig. 9). In fact, the summits of the fault blocks, some hundreds of meters above the valley floors, are flattened. It is easy recognizable because the sedimentary successions are tilted and the erosional surfaces clearly cut the strata. This flat erosional surface, usually slightly dipping northward, can be traced from block to block down to the feet of the escarpment. It suggests the existence of a pediment that in the past linked the main escarpment to the Afar depression floor. This surface also eroded many fault escarpments although locally it is cut by later fault activations (Fig.10). In this case, geological and geomorphological displacements do not coincide being the former always higher than the latter. To the latter we associate also the tilting of some flat remnants at the feet of the major faults. However, for any single fault we are able to distinguish a **pre-pediment** from a **post-pediment** period of fault activity. At the feet of the escarpment this surface is covered by the AFB (Fig. 11 and 12) and, if the radiometric age of 0.64 Ma (Audin et al., 2004) is correct, it would constrain the period of the later tectonic activity.

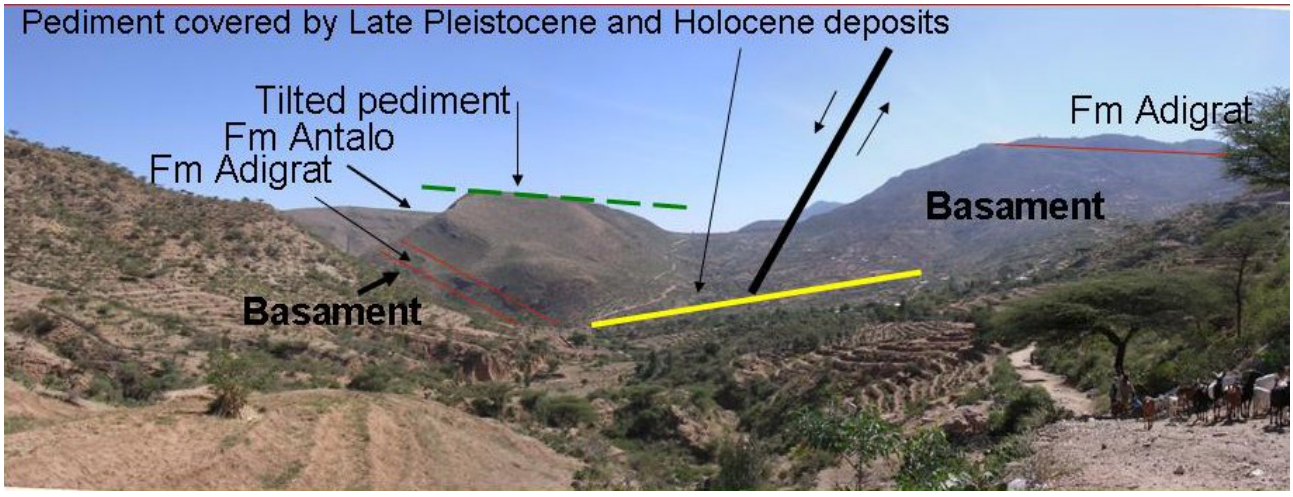

Fig. 9. *Main Escarpment. The sedimentary succession is faulted and tilted up to 60°, A long pediment affected the area before the deepening of the present-day drainage pattern and it has been lately tilted. another pediment modelled the foot slope during the Early part of the Late Pleistocene and it is covered with fluvial deposits.*

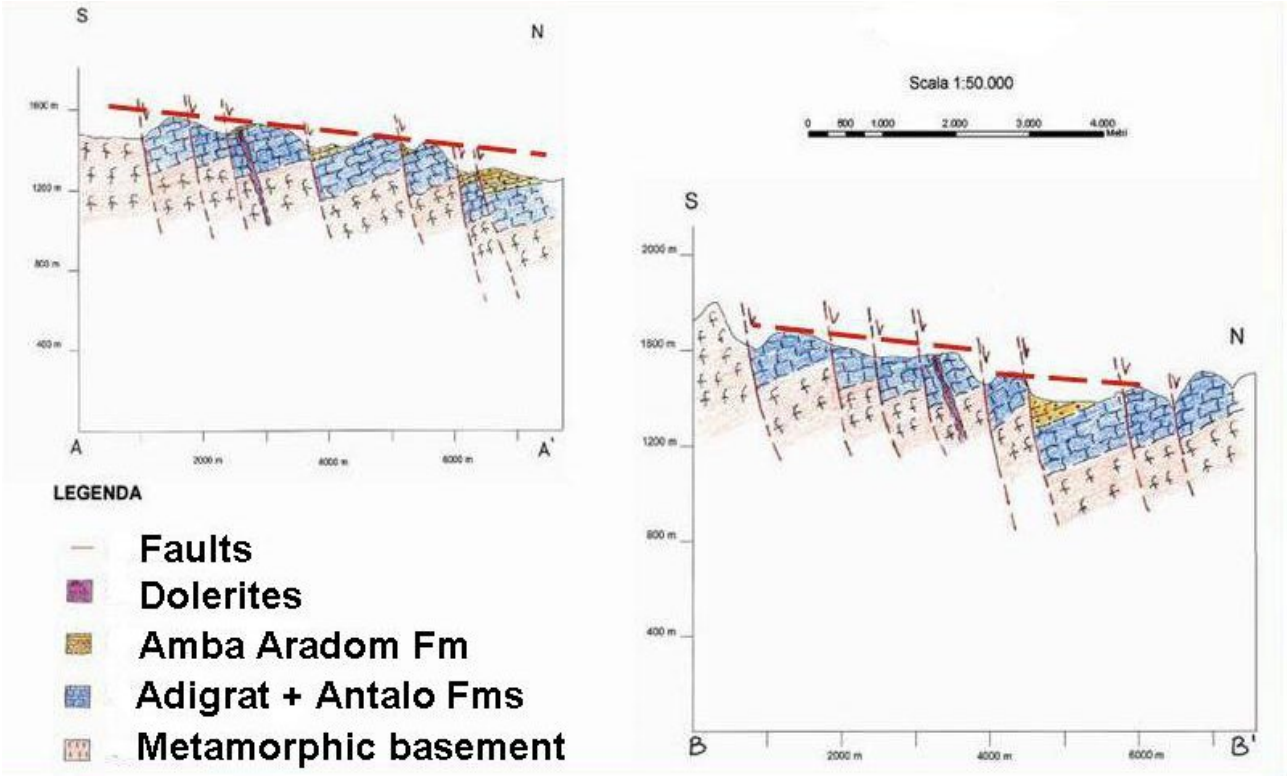

Fig. 10. Geological cross section showing examples of: a) pre-pedimentation faults; b) post-pedimentation faults.

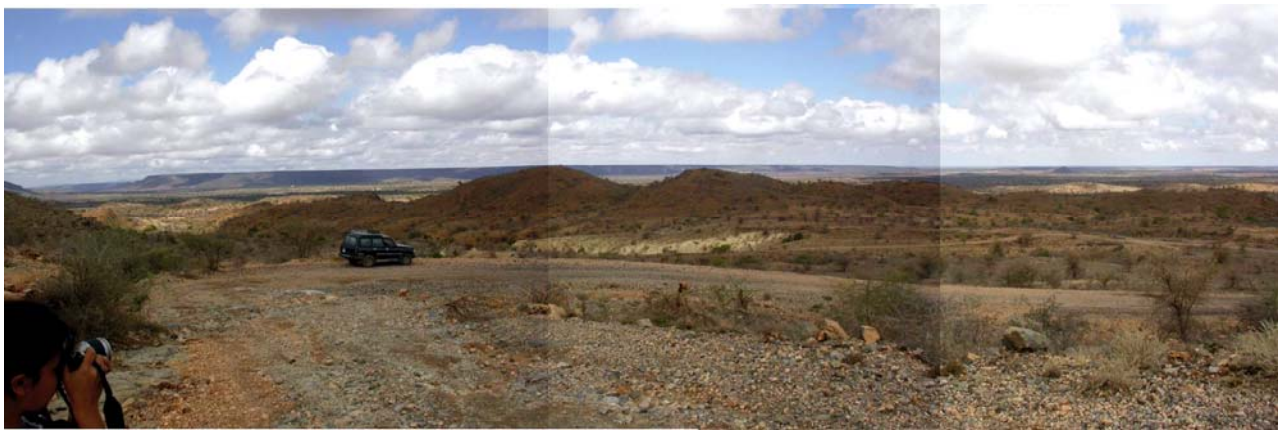

Fig. 11. A panoramic view of the Afar Stratoid Basalts on the foreground.

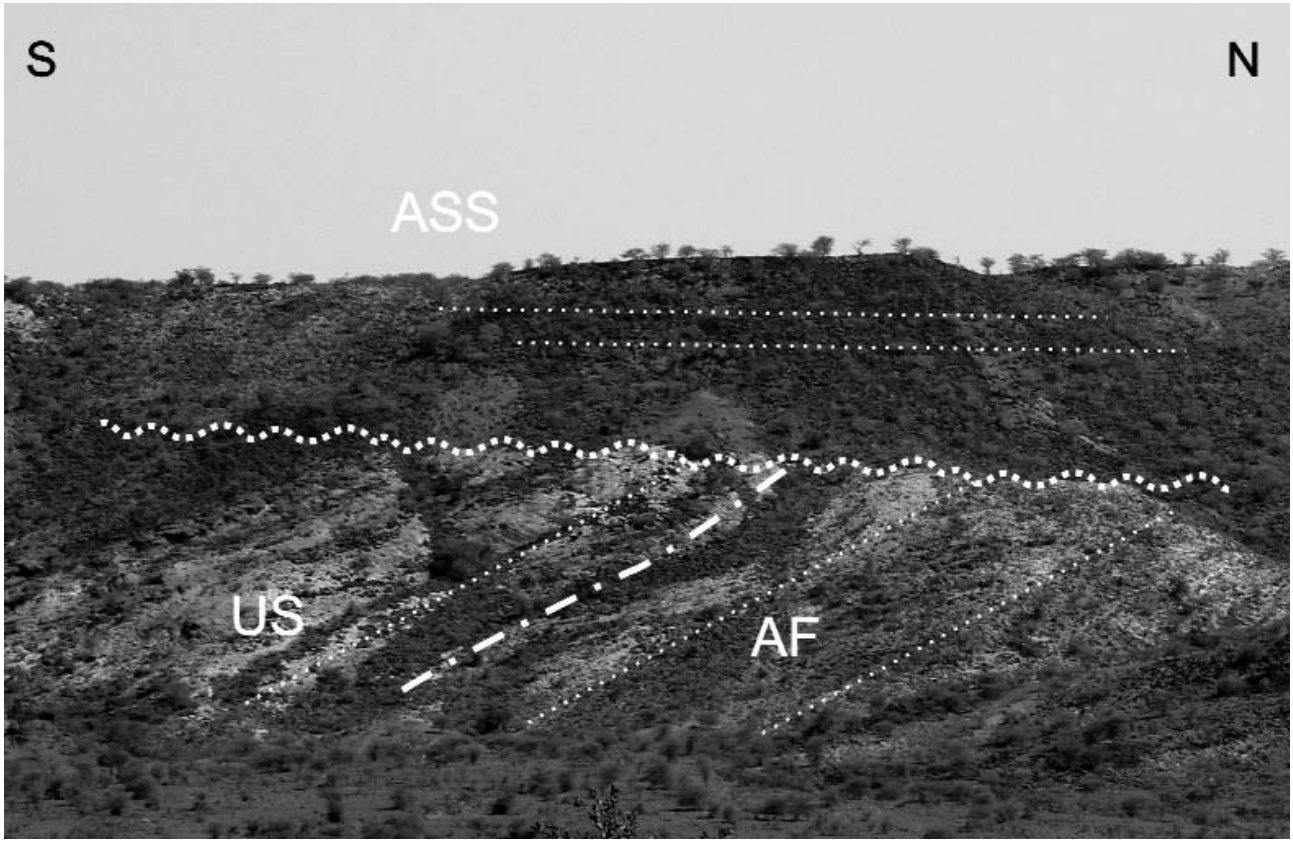

Fig. 12. The wavy line points out the unconformity surface at the top of the S-tilted fault block sealed by the basalts of the Afar Stratoid Series (ASS). Dashed line shows the trend of the bedding and dashed-dotted line outlines the boundary between the Antalo Fm. Limestones (AF) and the Upper Sandstones (US).

The evidence suggest that the modelling occurred during a long lasting arid period because there are no evidence of different orders of terraced pediment. However, these findings question the velocity of pedimentation processes commonly associated to arid conditions. In fact, although long period of arid conditions prevailed during the cold periods of the Middle Pleistocene they were already interrupted by climatic ameliorations.

The later valley downcutting dismembered the pediment and led to the present day morphological setting. The incision, in places more than two hundreds meters deep, was interrupted by the formation of a younger pediment (Fig.13) modelled during the arid phases of the Late Pleistocene, possibly during MIS 4 although there are still few dates to confirm it on a larger scale.

Fig.13. A pediment preserved at the foot of one of the main escarpment. It is usually covered by a veneer of gravels and sands and locally, close to the valley mouth, by calcareous tufa.

The Late Pleistocene pediment was later covered by two unconformity bounded stratigraphic units (UBSU; Salvador, 1994) made by different alluvial deposits. We investigated in details the stratigraphic setting, the sedimentological characteristics and the different facies of these deposits. Many organic layers and organic buried paleosoils were dated with radiocarbon and this allow us to establish the chronology of the events and the major environmental changes that affected the area since the Late Pleistocene. The two UBSU are named respectively Berak and Uadi Adakaloya, following the type sections (Sect. 120 and 200-199 respectively) and their C14 radiometric ages. A phase of incision separate the two UBSU and the older, although deeply dissected, locally generate an alluvial terrace with an upper depositional surface that, when preserved, is 10-15 m above the valley floor. Usually the Berak is also buried under the Adakaloya UBSU and the radiocarbon dates have been always obtained in this stratigraphic setting. To describe the alluvial deposits we followed the classification of Miall (1985; 1996) while for the calcareous tufa that of Golubic et al. (1994) and Ford & Pedley (1996) modified.

The Berak UBSU (Fig.14) is made of alluvial sands and gravels. At Berak (section 120) the older part of the succession, 6 m in thickness, rest on dolerites. It is made of massive and through cross

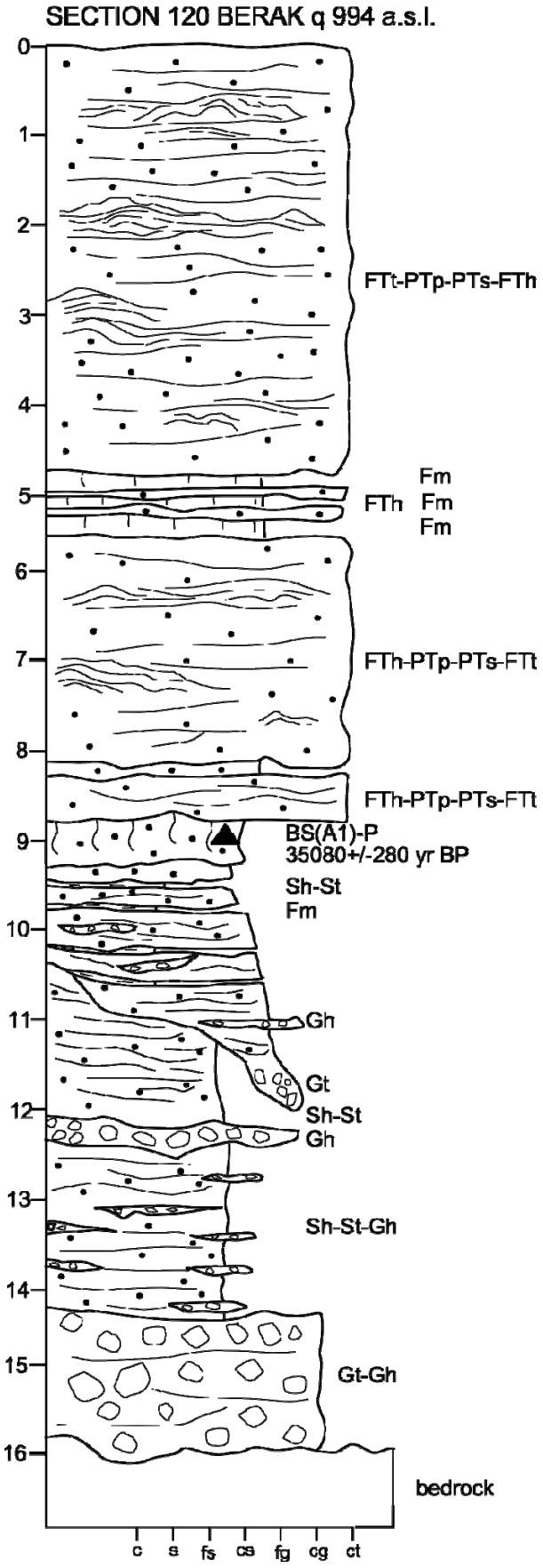

Fig. 14. Stratigraphic section 120 Berak with the facies interpretation: FTt, trough cross bedded phytoclastic tufa; FTp, planar cross bedded phytoclastic tufa; FTh, horizontal cross bedded phytoclastic tufa; Ptp, phytohermal tufa; PTs, phytohermal and phytoclastic tufa;
OTo, Oncoidal Tufa; MTm, micritic lacustrine tufa; Gt, trough cross bedded gravels; Gh, horizontal layered gravels; St, trough cross bedded gravels; Fm, massive mud; D, debris; S, soil; BS, buried soil; P, peat; ▲, radiometric age

bedded gravels (Gh, Gt) and horizontal and very flat trough cross bedded sands (Sh, St). A deep channel split in two parts the sequence that is covered by an Bwk organic rich soil with fine prismatic structure and pseudomicelia that gave a conventional age of 35.080 ± 280 yr BP (all reported dates are conventional). It is buried under the Uadi Adakaloya UBSU made by over 8 m of phytoclastic (Ft), phytohermal (PTp) and phytostromatic calcareous tufa (PTs).

The clastic sedimentation of the lower part of the sequence is associate to a period of slope degradation and river aggradation during the first half of the Last Glaciation (late MIS 4). The dated soil indicate a climatic amelioration that induced the growth of a forest-steppe environment. This created, at least at local scale, a relatively short interruption of the gravel sedimentation during MIS 3. The later part of the sequence that embraced the MIS 2 was completely cancelled in this section.

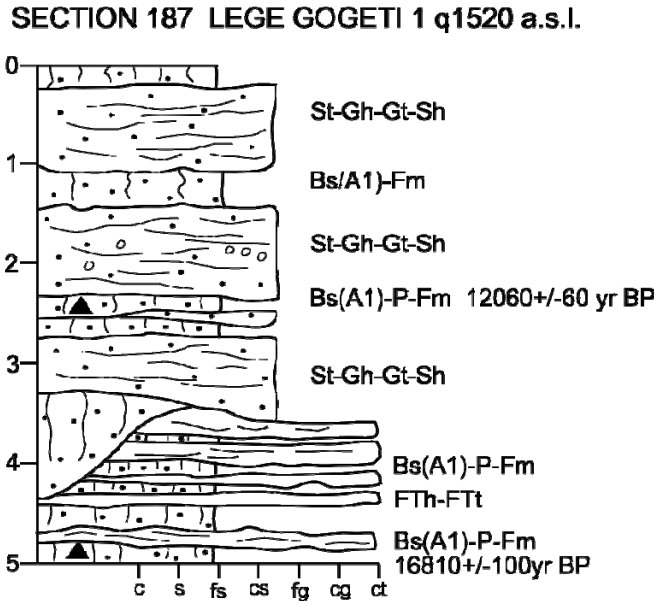

Fig.15. Stratigraphy of the Lege Gogeti 1 (Section 187) and (above) details of the lower part of the sequence buried under alluvial gravels and sands

Another section was found at Lege Gogeti 1 (Fig. 15) and possibly 2 (section 187 and 188) located a few hundreds meters apart. In fact the A1 organic horizon of a vertisols at the base of the sequence gave a conventional age of 16.810 ± 100 yr BP and another organic horizon on top of the lower part of the sequence was 12.060 ± 60 yr BP. These dates bracket a succession of phytoclastic calcareous tufa and thin palustrine organic mud with weak evidence of weathering. They were deposited during a climatic amelioration of the Late Glacial, possibly during Termination 1 (Johnsen et al, 1995) that correspond to the Allerod-Bolling of the North European pollen zone. The sequence indicate that during this time interval the slopes were covered by a thick vegetation cover and no slope

denudation processes were at work. Unfortunately this is the only sequence where calcareous tufa are dated to Late Glacial and it should be confirmed by further dating. However, it would be not surprising that along the border of the Afar this Interstadial corresponded to a strong climatic amelioration because this, naturally with different effects, was already recognised in northern Europe where the braided rivers of the Pleniglacial assumed a meandering pattern (Vandenberghe, 2002). The upper part of the succession is made of gravels and sands that could be partly related to the climatic worsening of the end of the Last Glaciation or to the late part of the Uadi Adakaloya UBSU that sometimes is represented by similar sediments.

Fig.16. Lege Hida (section 108)

Many other sequence containing calcareous tufa were dated in the study area. At Lege Hida (section 108; Fig.16) the organic horizon of a soil buried under phytoclastic calcareous tufa gave a conventional age of 9.120 ± 50 yr BP. It rest on trough cross bedded boulders, gravels and sands most probably belonging to the Berak UBSU. However, in this case the date simply indicate that the deposition occurred after this age. Better chronological constraints come from Uadi Adakaloya 1 (section 199, Fig. 17) and 2 (Fig.18, section 200). In the former the clastic succession, made of channelized trough cross bedded gravels with a boulder channel lag, are incrusted with phytostromatic tufa.

The upper part of the sequence is made of interlayered phytoclastic, phytohermal and phytostromatic layers (PTs, MTm) with some thin layers of organic rich palustrine mud. One organic layer covering a sequence of cross bedded sands with rare trough cross bedded gravels (St, Gt) gave a conventional age of 8.850 ± 50 yr BP that indicate that tufa deposition started again during the Early Holocene.

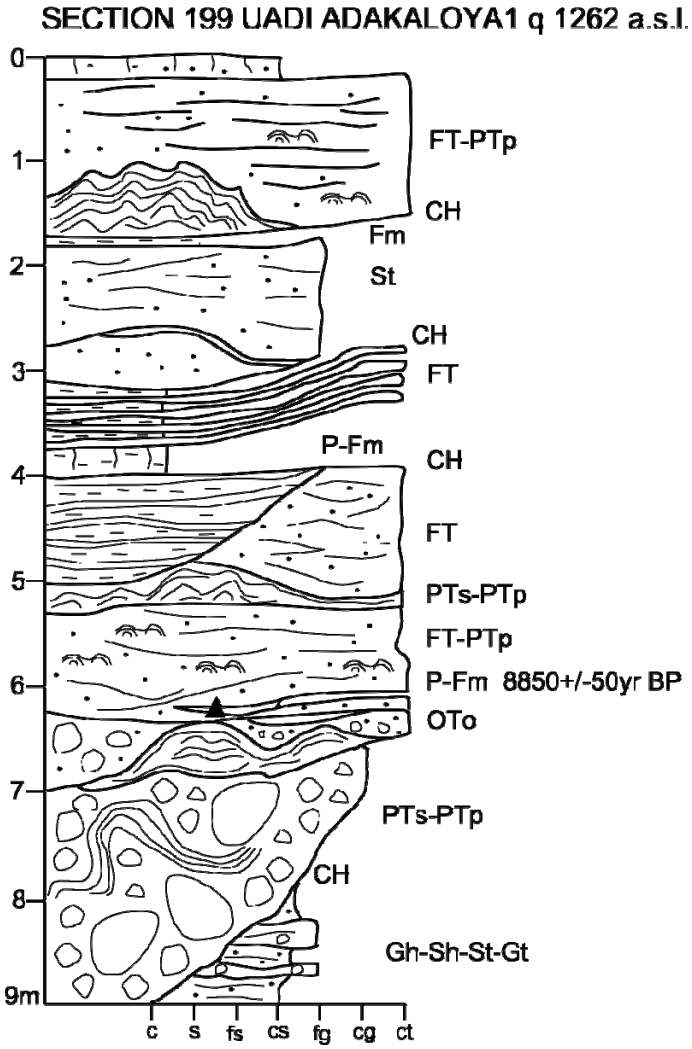

Fig.17. Stratigraphy, facies analysis and photo of the Uadi Adakaloya 1 (section 199).

A setting similar to Uadi Adakaloya 1 is found at Gende Dima (section 190) where the deposition within channels of phytoclastic tufa interlayered with palustrine mud already started before 8.900 ± 50 yr BP and surely was active at 8.130 ± 50 yr BP.

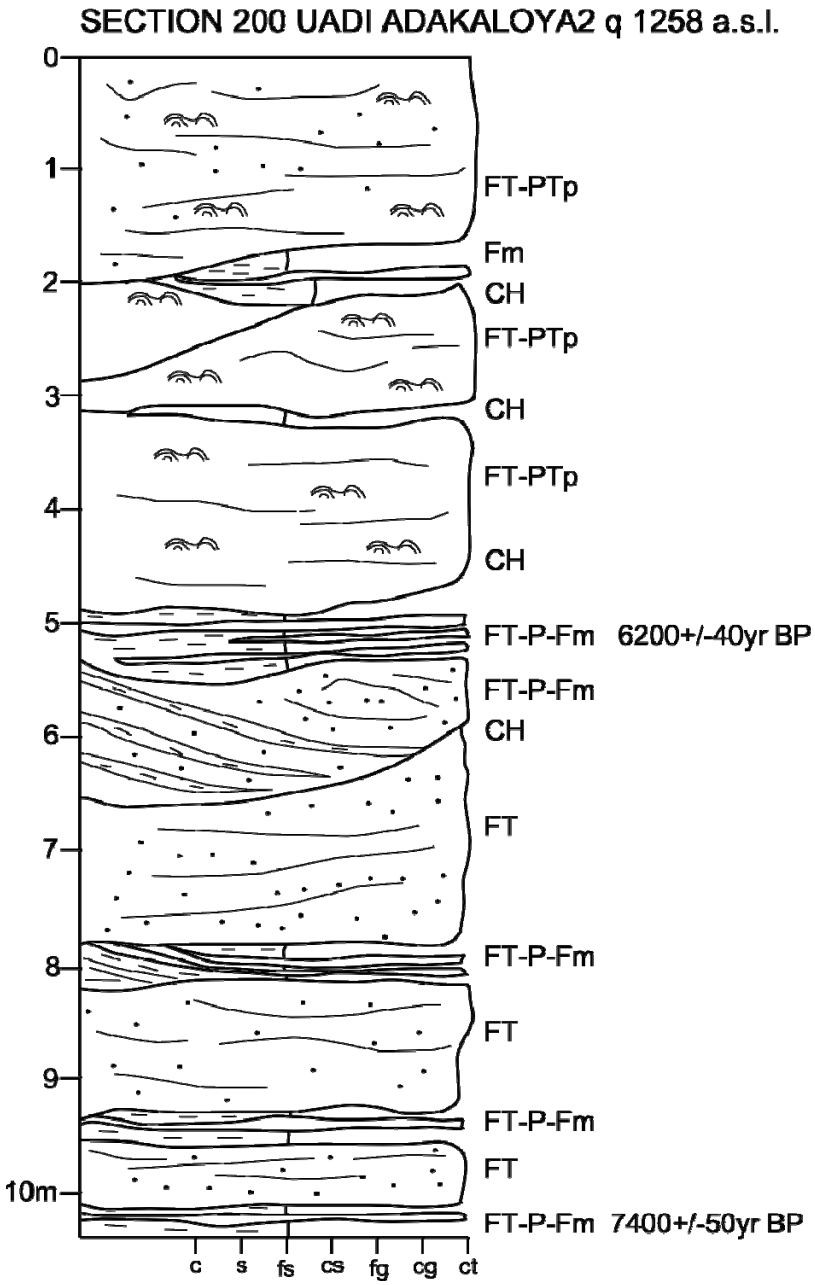

Fig.18. Panoramic view (above) and schematic section (below) of Uadi Adakaloya 2 (section 200)

Uadi Adakaloya 2 (section 200) is made at the base by phytoclastic sands interlayered with gravelly calcareous tufa and thin layers of palustrine organic mud. One of the lower

organic layers, gave a conventional age of 7400 ± 50 yr BP. The upper part of the succession is made by planar phytoclastic sands changing upward to trough cross bedded phytoclastic sands with thin phytohermal patches deposited within large channels again with some intercalation of organic muds. An organic layer buried under the upper channel gave an age of 6.200 ± 40 yr BP. In this area the top depositional surface of the calcareous tufa is well preserved. In other successions the beginning of the deposition of calcareous tufa started much later than at Uadi Adakaloya. However, this might also depend upon the position of the succession in the framework of the valley aggradation. At Hula Hulul (section 43) for example, phytoclastic tufa resting on coarse alluvial gravels and boulders were deposited after 6.510 ± 50 yr BP. At Lasdere 1, the sequence is made of trough cross bedded and horizontally bedded gravels and sands interrupted by organic rich soil horizons with a conventional age of 7.140 ± 40 yr BP.

At Gola Adada (section 65) organic rich layers at the bottom of a gravelly channel cutting phytoclastic tufa interlayered with palustrine weathered mud is dated at 6.620 ± 50 yr BP and suggests that the deposition of tufa had already ended.

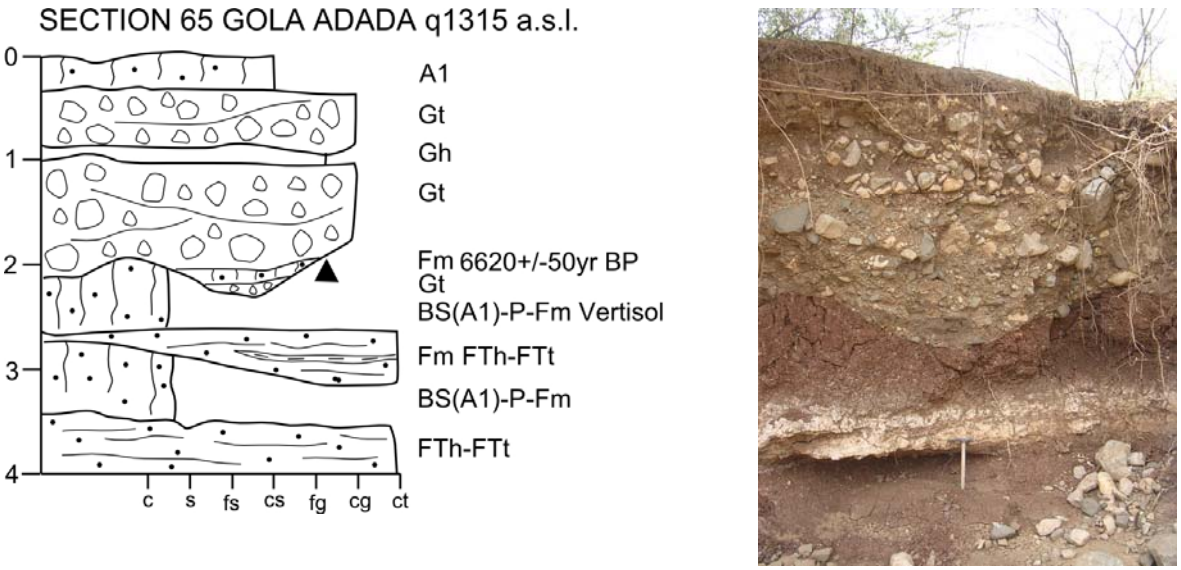

Fig. 19. Gola Adada Section

The relationship between stratigraphy, facies analysis and radiometric age shows that calcareous tufa deposition probably started already during the Termination 1 (Late Glacial), was possibly interrupted during the latest part of the Late Glacial and than started again at the beginning of the Holocene, around 9.000 yr BP. During the Middle Holocene their deposition ended everywhere although not synchronously. In some valleys, such as Uadi Adakaloya, the deposition continued well after 6.200 yr BP while in nearby valleys, such as Gola Adada and Lasdere 1, it was already replaced by coarse gravels and sands at 6.620 and 7.100 yr BP respectively. In Tigray, our investigations on the fluvial succession, including calcareous tufa, showed that tufa deposition ended after 5.200 yr BP, much later than in the Dire Dawa (Brancaccio et al., 1997; Berakhi et al., 1998).

The beginning of the deposition of calcareous tufa has been associated with the reforestation of the area firstly during Termination 1 and later during the Early Holocene that led to the stabilization of slopes and to an abrupt shortage of sedimentary load in the water courses. It is worth mention that deposition of tufa needs waters enriched with CO_2 that mostly come from the decay of organic matter. The tufa deposition is also largely associated with the activity of algae that are very sensitive to the clearness of the water. Waters plenty of mud are not consistent with tufa deposition. Therefore to bring the tufa deposition to an end it would necessary an abrupt reduction of the vegetational cover. It might be associated both to climate or to human impact, following the introduction of the early agriculture and pastoralism. We expect that climate changes would have an almost simultaneous effects on the area while our dating indicate that there is a long delay from one valley to another. Moreover it is difficult to assume that climatic changes would have eliminate the forest cover from the higher part of the slope where precipitation are quite abundant also nowadays (over 700 mm/yr). The fact that the area sustain a widespread agricultural activity suggests that also nowadays the potential vegetation would be a forest. These are the reasons why we strongly support a human induced deforestation as the main factor triggering the decline of calcareous tufa precipitation.

The lakes of central Afar, during the early Holocene up to 7 ka BP were at their maximum expansion and were, are dominated by chemical and biochemical sedimentation (Gasse et al., 1974). Due to the absence of clastics these authors suggested that the water supply came mostly from ground waters but our finding shows that this was probably the result of the growth of the forest cover.

Since Mid Holocene, after a period of gravel deposition that locally covers the calcareous tufa the sequence was eroded down to the present day river bed.

To summarize, during the fieldtrip we shall visit a landscape resulting from major drainage inversions generated by the activation of the normal faults delimiting the southern border of the Afar depression. The erosional processes affected a 20 to 30 km long escarpment made of 10 to 15 almost parallel normal fault segments that in place join each other and locally also diverge obliquely cutting for some kilometres other segments. The staircase of faults also included a series of secondary graben and horst. Their displacement it is easy to establish due to the presence of lithological key beds. A phase of pedimentation bevelled all the structures and constituted the starting point for the present day angular drainage pattern.

Fig.20 Calcareous tufa waterfalls generated large dam across the valley.

The growth of phytostromatic tufa along the waterfalls (Fig.20) generated a series of clinostratified, sometimes almost vertical, layers. Up valley they created a series of small ponds sometimes filled with fine calcareous whitish mud locally interlayered with dark organic layers. Down valley it is possible to find phytoclastic tufa and locally small phytohermal patches generated in correspondence of small cluster of vegetation. The deposition of tufa is locally replaced by coarse gravels and sands before the overall river downcutting responsible for the terracing of the older deposits. The calcareous tufa and the overlying sands and gravels are today hanging up to 10 m above the valley floors and usually are not reached either by the extraordinary floods. The deposit of the valley bottoms are nowadays made of sands and gravels within river beds usually slightly incised

in the two older UBSU. No deposition of calcareous tufa has been found in the area in correspondence with the major springs except fo very limited patches,

2nd day, February 14th: Departure from Awash and arrival in the Dire Dawa area around 11-12.

Stop 1: **Lange**: Yabeta Lencha area where small lakes (Fig.21) are preserved along the regional watershed at the head of the rivers that drains to the south (Fig.22).

Fig. 21. The edges of a lacustrine area along the watershed near Lange.

Fig.22. The morphology of the valleys draining to the south. The flat area at the top of the valley is a structural surface modelled over the Mesozoic rocks. Along the slopes there are a series of steps in correspondence of the more resistant layers. On the foreground the Gara Muleta made with the continental flood basalts

Stop 2: **Eastern slope of the Gara Muleta.** The Trap sequence (Oligocene Flood Basalts) is preserved up to 3500 m in elevation (Fig.23). Along the road is possible to see the sedimentary sequence resting above the metamorphic basement rocks cropping out in the deeper part of the valley. They are characterized by horizontally layered sedimentary successions separated by major unconformities that generated a stepped morphology due to selective erosion. With good weather we could also see, about 65 km to the east, at Jijiga, the remains of another relief made of the CFB. These are the easternmost outcrops in the area and give an account of the deepening of the drainage network before the onset of the rifting. Over 1500 m separate the top of the Gara Muleta (3.550 m)

Fig.23. The relief of the Gara Muleta modelled over the Continental Flood Basalts. The flat surface of the secondary watershed that are visible at lower elevation is the re-exumation of the unconformity cutting the Jurassic rocks.

Fig.24) Large scale gravitational movements generating long tranches and counter-slope blocks.

from the Lange area (ca 2000 m) that represented the uppermost remain of the pre-Rift valley bottom. The slopes modelled over the basalts have a stepped morphology due to the presence of different lava flows. The slope is affected by very large gravitational movements evidenced by long trenches and widespread counter slopes and bedrock deformations (Fig.24). Along the road that cross the main escarpment to Dire Dawa we shall see a large dolerite dike slightly evidenced by selective erosion. Further down, before reaching Dire Dawa, we shall see a series of EW fault angle valleys. In one of these valleys selective erosion affected a dolerite laccolite.

Stop 3: Kaderse Ade. Fault escarpment at the southern border of the Afar plain. A pediment (Fig.25) is sculptured at the feet of the escarpment locally covered with a veneer of alluvial sediments and calcareous tufa that we shall face in detail the next day.
The Jurassic rocks are affected by a dragging associated with the faulting (see fig. 8). The Afar depression continue to the north with some volcanoes rising along the plain located at an elevation of ca. 1000 m. To the northwest it is possible to see the Afar Flood Basalts that generate a mesa landscape. The photos of fig. 12 was taken at the feet of the mesa. Along the road we shall visit the valleys developed at the feet of the secondary fault escarpment. One of them is again modelled on dolerite laccolites and sills.

Fig.25 Pediment modelled at the feet of the lower escarpment bordering the southern margin of the Afar depression.

Overnight in Dire Dawa

3rd day, February 15th

Fig.26. General view of the fault escarpments in the Hulul area

Stop 1: <u>Lege Oda Mirga</u>: Staircase of fault escarpment along the border of the Afar (Fig. 9). At the feet of the main escarpment, at the top of the relief, we observe the Middle Pleistocene terraced pediment (fig.13). The layers are dipping ca. 20-30° to the south while the pediment, that once was dipping few degrees to the north, has been rotated by the reactivation of the normal fault and now dips few degrees to the south. This allowed to distinguish between a pre-pedimentation and a post pedimentation fault activity. No fault activity occurred since the Late Pleistocene. A minor hanging valley contains calcareous tufa deposits that in the past generated a waterfall.

Stop 2: **Hulul**, General view of the fault escarpment in the Hulul area. The main escarpment (fig.26) is affected by trenches and deformations associated with deep seated gravitational movements.

Stop 3. Section 190, Gende Dima: Thick sequence of calcareous tufa with different facies association. Radiocarbon dates on interlayered organic mud indicate that the deposition of tufa started before 8900 yr BP. This is one of the oldest Holocene deposits in the area. A date of 8130 yr BP in the middle part of the sequence allow us to evaluate the local depositional rates of the calcareous tufa.

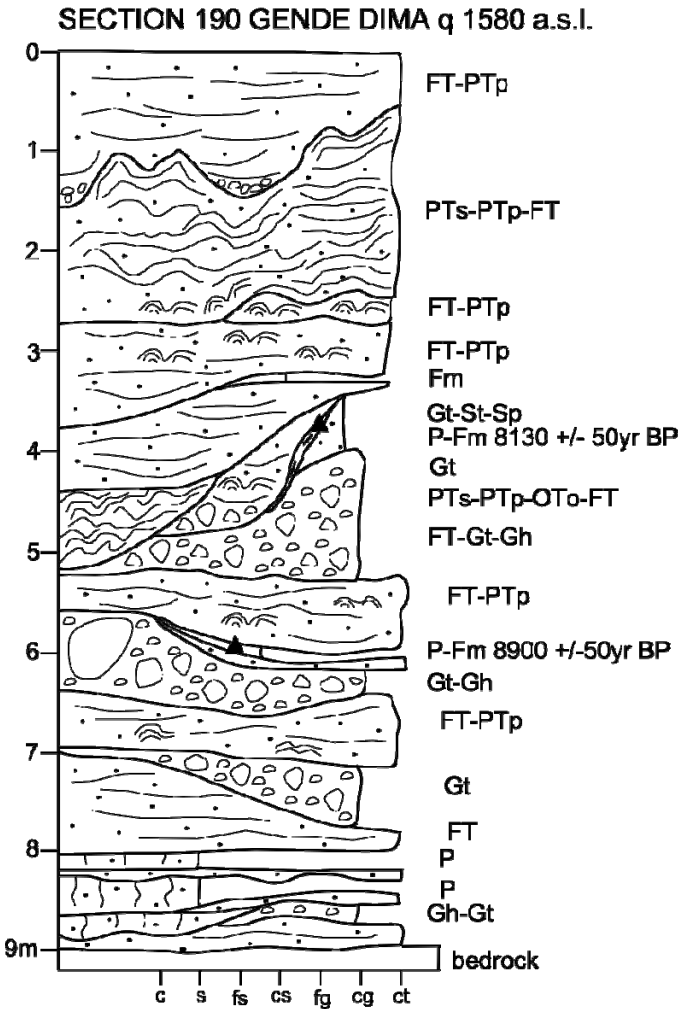

Fig.26. Section 190 Gende Dima: details of the upper part (above) and the lower part (below)

Stop 3: Lege Gogeti. A series of calcareous tufa crops out at Lege Gogeti. The section o Lege Gogeti 1 has been already illustrated in the previous part of the text (Fig. 27). We shall also visit Lege Gogeti 2 where the deposition is entirely represented by

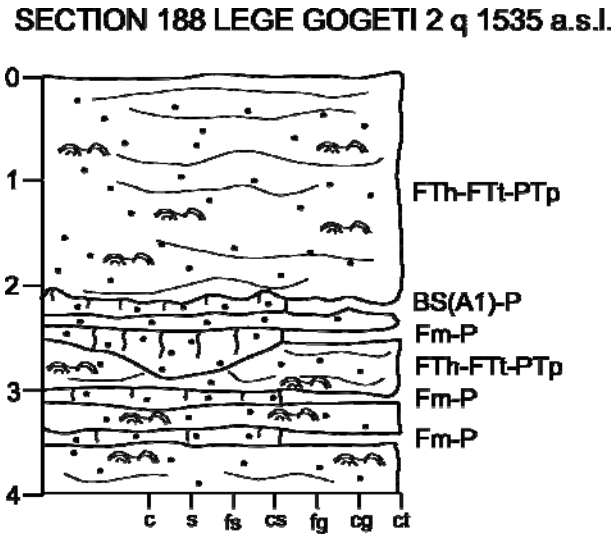

Fig. 27. Section of Lege Gogeti 2

calcareous tufa with intercalations of organic mud. Unfortunately no dates are available for these deposits that apparently should have similar ages that Section 1

Note: *This part of the guide has been realized thanks to the results of a geological and geomorphological mapping that was realized in 2006 and 2007 with the participation of Castellani A., Disperati L., Firuzabadì D., Gandin A., Pontarelli L., Sacchi G., Salvini R., Pizzi A. and Pomposo G. that we greatly acknowledge. Many thanks also to Pieruccini P. for the help and suggestions in preparing this booklet.*

Departure: overnight in Awash

4th day. February 16th

Stop 1: Gewane. At this stop, the Main Ethiopian Rift (MER) has already entered into Afar. We are on the W side of the MER. We are facing one of the easternmost active normal faults bordering the rift side. The recent activity of the fault is testified by the presence of a clear morphological scarp. The scarp also affects a spatter cone, downthrowing its westernmost portion. It is possible that the vent has been fed by a dike propagating along the fault, and later dissected by the activity of the fault itself.

Stop 2: Afar Stratoids. We are a few km to the SW of Tendaho Graben, in Central Afar. The area is characterized by the presence of the widespread and thick Afar "Stratoid" sequence, made up of flood basalts and ignimbrites, marking the transition to an oceanic crust, from 4 to 1 Ma; (Barberi et al., 1972; Barberi et al., 1975).

At this stop, it is possible to observe the cross-cutting relationships between the NW-SE trending structures of the Red Sea Rift, responsible for the development of the Tendaho Graben (TG), and the NNE-SSW trending structures forming the northernmost part of the Main Ethiopian Rift (MER). TG interrupts the continuity of MER, as suggested by the abrupt termination of the structures forming the latter. In fact, the northernmost MER structures in the TG area are found within the Afar Stratoids on the SW shoulder of TG. This termination of MER structures against TG structures and the lack of MER structures within and to the N of central TG indicate a drastic change in the tectonic conditions, probably controlled by the higher spreading rate (almost 1 order of magnitude) of the southern Red Sea Rift relative to the Main Ethiopian Rift.

This stop shows a small-scale example of these cross-cutting relationship (Fig. 28): the NNE-SSW trending normal fault, highlighted by a scarp, in the northern MER is displaced

by a NW-SE trending fault, highlighted by another scarp, on the TG shoulder. However, the foot-wall of the latter is slightly dissected by the MER fault, suggesting an almost contemporaneous, even though not comparable, activity of the two faults. As the Afar Stratoid sequence is not typically eroded in this desert climate, topography can be used as a reference to measure the offset of faults. While the northern MER faults have a predominant extensional component, the NW-SE fault has a predominant strike-slip activity, with a left-lateral component ~300 m and a vertical component ~20 m (Fig. 28).

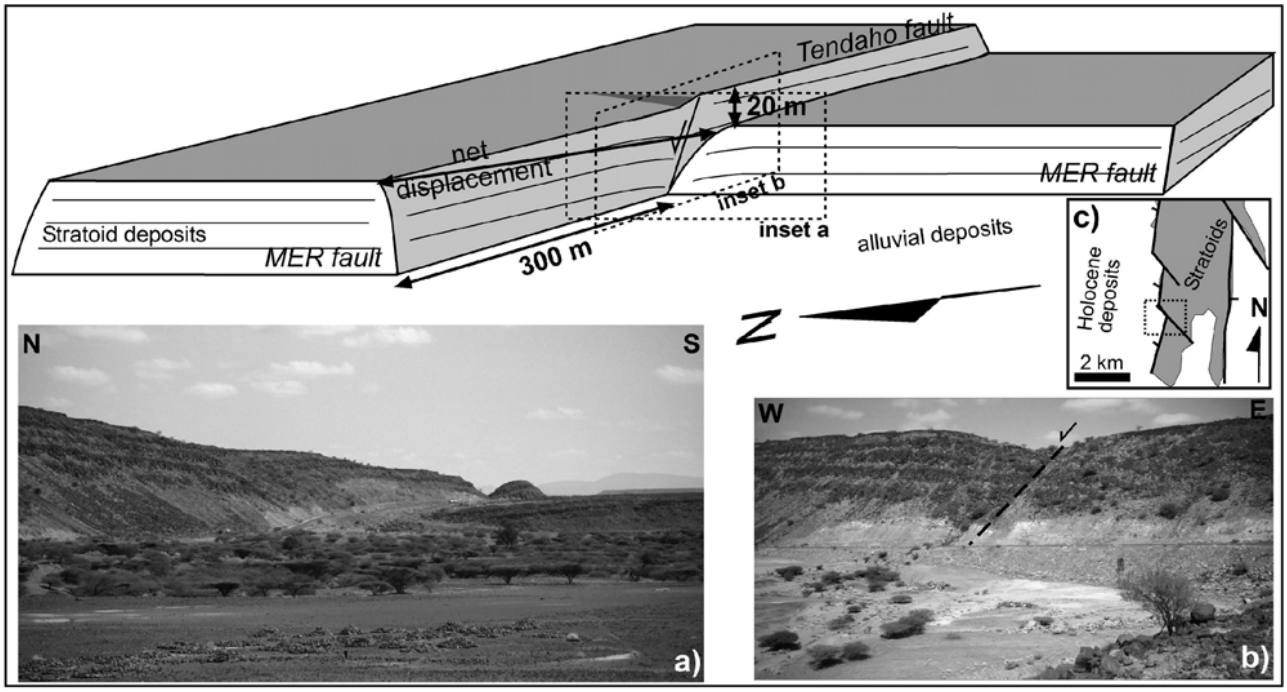

Fig. 28 – Example of cross-cutting relationships between the NNE-SSW trending MER structures and the NW-SE trending Red Sea structures (parallel to those of Tendaho Graben) (Acocella et al., 2008).

Stop 3: SW Tendaho Graben. TG is bordered by NW-SE trending faults, at all scales (Fig. 29). Remote sensing and field data show that the overall architecture of TG is characterized by the following features (Fig. 29). a) The NE and SW shoulders consist of subhorizontal Stratoid layers, often dissected by NW-SE trending faults. b) At the NE and SW graben margins, marked by the highest visible scarps, the subhorizontal Stratoid layers end, forming inward dipping Stratoid blocks arranged in a domino configuration inside the margins. The dominos, usually ~1 km wide, are bordered by NW-SE trending faults which dip away from the graben axis; the displacement of these faults decreases towards the graben axis, in a similar fashion to the amount of tilt of the blocks that they

bound (between 30° and 5°). c) Stratoids in the inner portion of TG are deformed into a broad NW-SE trending syncline-like structure (Fig. 29), formed by the tilted blocks separated by the NE-SW trending faults. Therefore, the syncline is fault-controlled and its axis represents the axis of TG. d) Thick (~1000 m) volcanic and sedimentary sequences are present within the TG; the youngest basalts (~300 to ~30 Ka) outcropping in its NE part mark the present active axis of Manda Hararo Rift. The spatial coincidence between the sharp topographic variations at the sides of TG (scarps >200 m high), the location of the tilted blocks, and sporadic hydrothermal activity suggest the presence of master faults bordering Tendaho Graben (Fig. 29). The foot-wall of the master faults is made up of Stratoids with subhorizontal attitude, whereas the hanging–wall is made up of tilted Stratoid blocks. Their vertical displacement does not only result from topographic variations (>200 m), but also from the tilt of the blocks on the hanging-wall. This accounts for a significant part of the ~1600 m of vertical displacement of TG calculated by means of drill data.

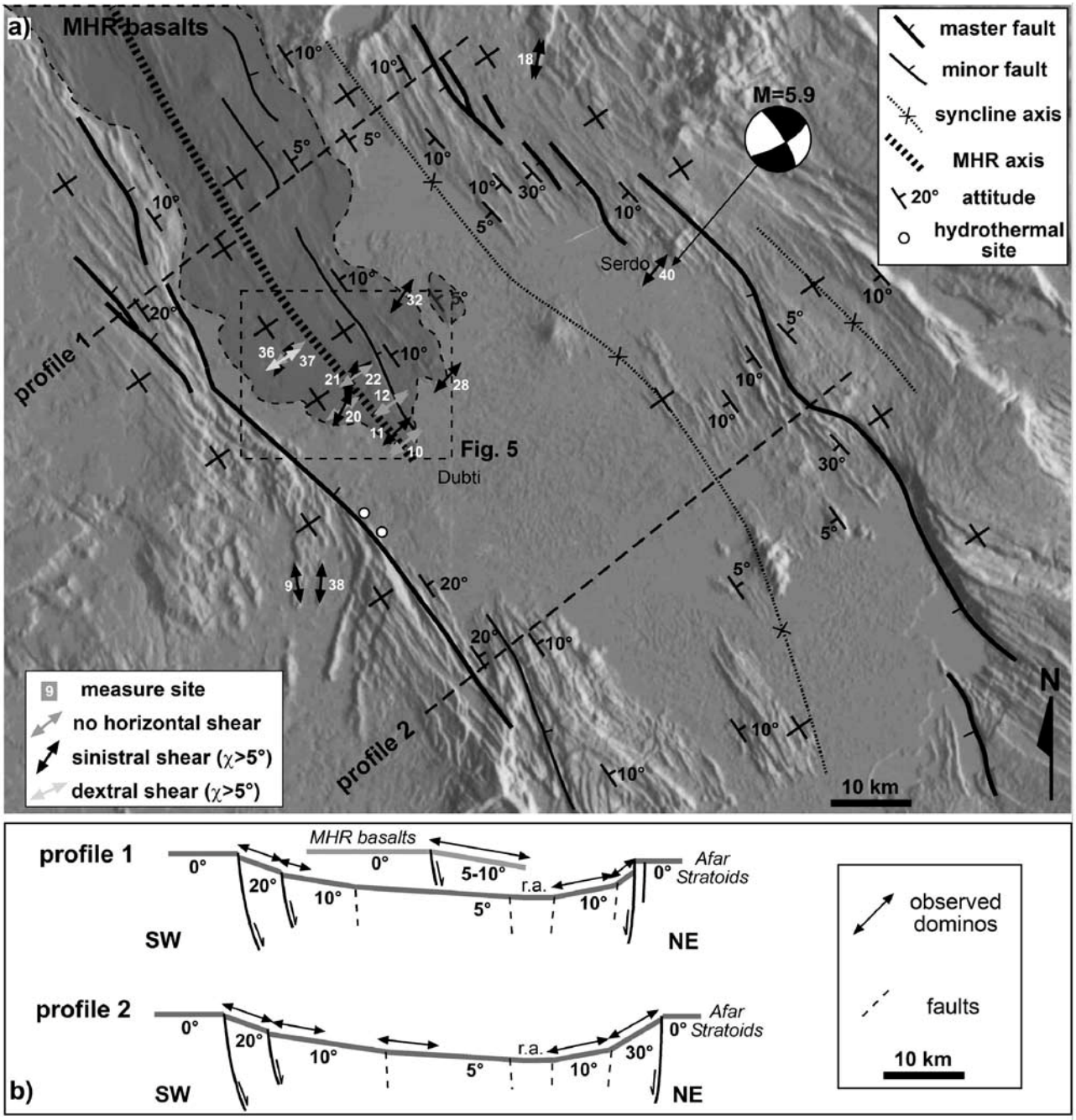

Fig. 29 – Simplified structure of Tendaho Graben, reposrting the main faults and the attitude of the Afar Stratoids (Acocella et al., 2008).

In this stop it is possible to appreciate the structure of the SW border of the Graben, where the border normal fault separates the subhorizontal Stratoids (outside the Graben) from the inward tilted Stratoids (inside the Graben) (Fig. 30).

Fig. 30 – SW border of Tendaho Graben, along the border normal fault. The picture is taken standing on subhorizontal Stratoids, immediately outside the Graben, looking at the inward dipping Stratoids blocks within the Graben.

5th day. February 17th

Stop 1: NE border of Tendaho Graben. In this stop it is possible to appreciate the structure of the NE border of the Graben, where the border normal fault separates the subhorizontal Stratoids (outside the Graben) from the inward tilted Stratoids (inside the Graben). The overall structure represents the mirror image of what observed at Stop 3 of day 4, on the SW border. Therefore, considering the stops at both sides of the Graben, the overall structure of the relatively symmetric depression can be appreciated. This results bordered by two-oppositely verging normal faults, separating an outside domain, where the Stratoids are subhorizontal, from a domain within the Graben, where the Stratoids forming the basement of the Graben form oppositely-facing inward tilted blocks.

On this NE side of the Graben, a M=5.9 earthquake (epicentre in the village of Serdo; Fig. 29) occurred in 1969. The earthquake induced surface fracturing, partly still visible today.

Stop 2: Manda Hararo Rift. This stop is located along the S tip of the NW-SE trending Manda Hararo Rift, which marks the termination of the presently active Red Sea Rift in Central Afar. A few km to the NW (Dabbahu area), a rifting event has been ongoing from 2005. The event was characterized by repeated intrusions of magma, through dikes, intruding a portion of rift >60 km long, and separating its two sides of >8 m (Wright et al.,

2006, Sigmndsson, 2006; Hamling et a., 2010). This intrusive process allows understanding the mechanism of divergence between two plates. Our stop is located exactly on the S continuation of the rifted area, along the axis of the rift, characterized by NW-SE trending extension fractures and open normal faults. These are the surface expression of the current divergence between the Arabia and Nubia plates, within the Tendaho Graben. Here the new capital of the Afar region, Semera, has just been built. The town itself is located exactly on the rift axis, above the active fractures and faults. This stop allows appreciating the active tectonic structures forming the rift axis and affecting Upper Pleistocene basaltic lava flows (Fig. 30). The open normal faults are similar to those observed in Fantale, though smaller. In addition, extension fractures, with a maximum opening in the order of a meter, are widespread and mark the exact location of the rift axis.

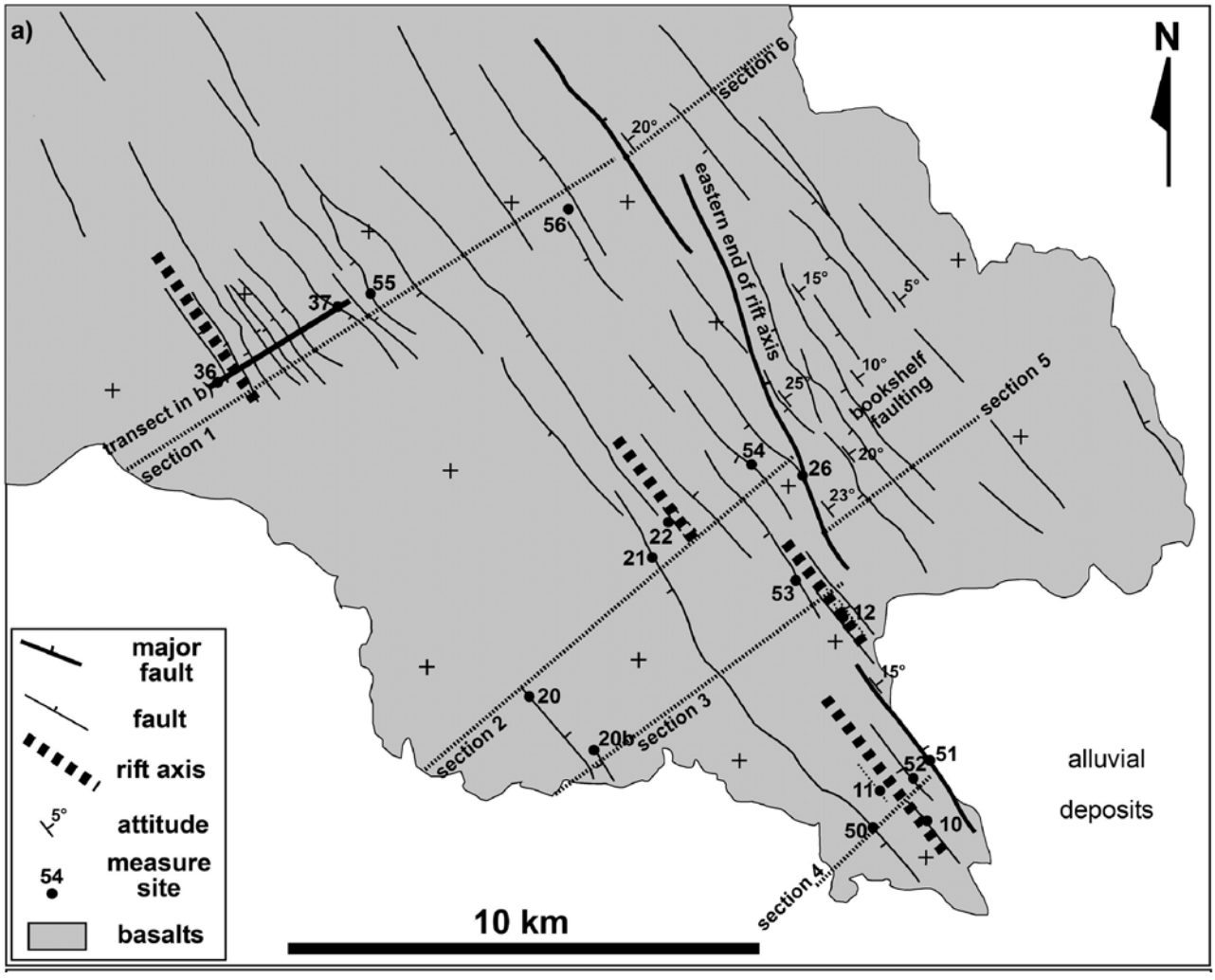

Fig. 30 – Simplified structure of the Manda Hararo Rift, in the area of Semera (SE part of the figure). The Upper Pleistocene basalts, fractured and faulted, are surrounded by the younger alluvial deposits (white) (Acocella et al., 2008).

5th day. February 16th

Coseismic surface faulting in the Kara Kore area (Wollo) caused by the May 29, 1961 Earthquake

(*mostly taken from Gouin, 1979*)

G. FUBELLI & F. DRAMIS

Department of Geological Sciences, "Roma Tre" University, Rome, Italy

1. The May 29, 1961 Kara Kore Earthquake

In 1961, from the end of May to the end of September, over 3500 earthquake shocks were recorded from the Kara Kore area at the Geophysical Observatory in Addis Ababa. A first series of earthquake shocks, which began on 29 May, reached a maximum frequency of 150 per day; a second series began on 1 June with a peak frequency of 350 per day. Two shocks had a magnitude >6.4 and seven >5.0. The felt area was estimated as about 300,000 km^2 and a relatively higher intensities were observed in the southeastern sector of the zone. The maximum intensity at the centre of the epicentral zone was estimated as VIII-IX on the Mercalli-Modified scale.

Cracks, fissures, and subsidence of up to 1 meter deep developed on the Addis Ababa - Mekelle highway: many culverts and retaining walls along the road had to be rebuilt. Gravitational movements were observed on steep escarpments slopes and a 15-20 km long fissure, in places 6-7 meters deep, formed in unconsolidate soil along the eastern scarp of the Borkena marginal graben (Fig. 1). There were no casualties.

Figure 1. *Panoramic view of the Borkena graben in the Kara Kore area. Coseismic deformation affected the road on the right of the image during the 1961 earthquake.*

The maximum damage was localized along the Addis Ababa – Mekelle highway between latitude N10° and 11° and longitude E 39.7° and 37.9°. At these latitudes, the highway runs along the upper margin of the eastern escarpment of the Ethiopian Plateau, which is dissected longitudinally by the Borkena graben, and transversely by NE-SW faulting curving in from Afar. In the epicentral area, the village of Majete was completely destroyed while the village of Kara Kore was affected only in part, maybe because of the type of buildings. In Kara Kore

only the masonry collapsed, while the tukuls withstood the shocks very well. Along the highway, damage was spectacular. Large boulders from rockslides, some estimated to weight 12 – 15 tons, blocked the road. Bridge pillars were fissured and parapets destroyed; cracks as wide as 60 cm and as deep as 150 cm were opened in the road surface; heavy slumping and subsidences with a resulting difference of some 100 cm in the surface level rendered the road impassable. All the bridges and culverts between kilometre posts 240 and 255 from Addis Ababa had to be rebuilt. Heavy alterations in the landscape had been also recognized. In addition to the numerous landslides, a piedmont scarp in unconsolidated materials opened along the escarpment of the Borkena graben. This scarp could be followed over 12 – 15 km until it became obscured by rubble. In some places, the vertical differential displacement reached 2 m, the depth 5-7 m, and the width at the surface over 1 m.

Excursion stops

Stop 1. ***Active fault on the Addis Ababa-Mekelle highway, south of Kara Kore***

A gravel quarry excavated on the Addis Ababa-Mekelle highway, few kilometres south of Kara Kore, on the eastern bordering scarp of the Hora basin, a small tectonic depression located on the southern edge of the Borkena graben (Fig. 2), makes it is possible to examine a north-south trending normal/strike slip fault that displaces Tertiary volcanics (footwall) and slope-alluvial deposits (hanging wall), referred to the Quaternary in the Geological Map of Ethiopia (Menghesa Tefera *et al.*, 1996). A trench running along the intersection of the fault with the ground indicates a very recent reactivation likely occurred during the May 29, 1961 (Gouin, 1979).

The deep incision of the downthrown sediments indicates that the fault displacements have acted in connection with the strong uplift that affected the area in Pliocene-Quaternary times (Faure, 1975; Almond, 1986; Mohr, 1986).

Figure 2. *Upper photo: quarry in the Kara Kore area where the contact between the basalt and slope/alluvial deposits due to the fault activity is exposed. Lower photos: detail of the slope*

deposits (left) tilted towards the fault plane (the white dashed line marks the attitude of the deposits) and (right) dragged (as indicated by yellow dashed lines) along the fault plane (indicated by red arrows).

Stop 2. ***Coseismic surface faulting at Kara Kore*.**

In this stop a showy surface fault produced in connection with the May 29, 2001 earthquake can be observed. At Kara Kore, on the eastern bordering slope of the Borkena graben, a piedmont scarp in unconsolidated materials is still visible. This scarp could be followed over 12 – 15 km with vertical displacement up to 2 m (Gouin, 1979). Considering that this displacement is very high in relation to the earthquake magnitude (M=6.6), it seems likely to explain it by the contribution of a strong gravity stress related to the high difference of relief between the Ethiopian Plateau and the Afar (Chorowitz *et al*. 1999).

Stop 3. ***Coseismic surface faulting at Majete*.**

Coseismic ground ruptures related to the 1961 earthquake are visible in the Majete area on the western side of the Borkena basin.

References

Almond D.C., 1986. *Geological evolution of the Afro-Arabian dome*. Tectonophysics 131, 301–332.

Audin L., Quidelleur X., Coulie E., Courtillot V., Gilder S., Manighetti I., 2004. Paleomagnetism and K-Ar and 40Ar/39Ar ages in the Ali Sabieh area (Republic of Djibouti and Ethiopia). Constrains on the mechanism of Aden ridge propagation into southeastern Afar during last 10Myr*. Geophys. J. Int*., 158, 327-245.

Acocella V., Korme T., Salvini F., Funiciello R., 2002. Elliptic calderas in the Ethiopian Rift: control of pre-existing structures. *Journal of Volcanology and Geothermal Research*, 119, 189-203.

Acocella V., Korme T., Salvini F. , 2003. Formation of normal faults along the axial zone of the Ethiopian Rift. Journal of Structural Geology, 25, 503-513.

Acocella V., Abebe B., Korme T., Barberi F., 2008. Structure of Tendaho Graben and Manda Hararo Rift: implications for the evolution of the Red Sea propagator in Central Afar. *Tectonics*, 27, TC4016, doi:10.1029/2007TC002236.

Acton, G.D., Tessema A., Jackson M., Bilham R., 2000. The tectonic and geomagnetic significance of paleomagnetic observations from volcanic rocks from central Afar, Africa, *Earth and Planetary Science Letters, 180,* 225-241.

Audin L., Quidelleur X., Coulie E., Courtillot V., Gilder S. Manighetti I., 2004. Paleomagnetism and K-Ar and 40Ar/39Ar ages in the Ali Sabieh area (Republic of Djibouti and Ethiopia). Constrains on the mechanism of Aden ridge propagation into southeastern Afar during last 10Myr*. Geophys. J. Int*., **158**, 327-

Berakhi O., Brancaccio L., Calderoni G., Coltorti M., Dramis F., Mohammed Umer M., 1998. The Mai Makden sedimentary sequence: a reference point for the environmental evolution of the Highlands of Northern Ethiopia. *Geomorphology*, 23, 127-138, Elsevier, Amsterdam.

Barberi F., Tazieff H., Varet J., 1972. Volcanism in the Afar depression: its tectonic and magmatic significance. *Tectonophysics*, 15, 19-29.

Barberi, F., G. Ferrara, R. Santacroce, J. Varet,1975. Structural evolution of the Afar triple junction, In: *Afar Depression of Ethiopia,* Pilger A., Rosler A. eds., Stuttgart, 1, 39-54.

Barberi F., Varet J., 1977. Volcanism of Afar: small-scale plate tectonics implications. *Geol. Soc. Am. Bull*., 88, 1251-1266.

Beyene, A., Abdelsalam M.G., 2005. Tectonics of the Afar depression: a review and synthesis, *Journal of African Earth Sciences, 41,* 41-59.

Brancaccio L., Calderoni G., Coltorti M., Dramis F., Ogbaghebriel Berakhi, 1997. Phases of soil erosion during Holocene in the Highlands of Western Tigray (Northern Ethiopia): a preliminary report. In Bard K. Ed., 'The environmental history and human ecology of Northern Ethiopia in the Late Holocene: preliminary results of multidisciplinary Project'*, Istituto Universitario Orientale*, 29-44, Napoli.

Bosellini A., Russo A., Assefa G., 2001. The Mesozoic succession of Dire Dawa, Harar Province, Ethiopia. *Journal of African Earth Sciences*, 32 (3), 403-417.

Chernet, T., Hart, W. K., Aronson, J.L., Walter, R.C. 1998. New age constraints on the timing of volcanism and tectonism in the northern Main Ethiopia Rift-southern Afar transition zone (Ethiopia). *Journal of Vulcanology and Geothermal Research*, 80, 267-280.

Cole, J.W., 1969. Gariboldi Volcanic Complex, Ethiopia. *Bulletin of Volcanology*, 33, 566-578**.**

Coltorti M., Dramis F., Ollier C., 2007. Planation surfaces in northern Ethiopia. *Geomorphology*, 89, 3-4, 287-296.

Coulié, E., Quidelleur, X., Gillot, P. Y., Courtillot, V., Lefèvre, J. C., Chiesa, S., 2003. Comparative K-Ar and Ar/Ar dating of Ethiopian and Yemenite Oligocene volcanism: implications for timing and duration of the Ethiopian traps. *Earth & Planetary Letters*, **206**, 477-492.

Ebinger, C.J., Hayward N.J., 1996. Soft plates and hot spots: views from Afar, *Journal of Geophysical Research, 101,* 21859-21876.

Ebinger C.J., Casey M., 2001. Continental breakup in magmatic provinces: an Ethiopian example. *Geology*, 29, 527-530.

Faure H., 1975. *Neotectonics in the Afar (Ethiopia, T.F.A.I.)*. In: Suggate R.P., Creswell M.M. (eds.), *Quaternary Studies*, R. Soc. New Zealand, Wellington, pp. 121-126.

Ford T.D., Pedley H.M., 1996. A review of tufa and travertine deposits in the world. *Earth.Sc.Rev*., 41, 117-175.

Golubic, S., Violante, C., Ferreri, V., D'Argenio, B., 1994. Algal control and early diagenesis in Quaternary travertine formation. Rocchetta a Volturno travertines (Central Apennines). *Bollettino della Società Paleontologica Italiana*, Special Volume, 1, 231–247.

Ghebreab W., 1998. Tectonic of the Red Sea Region reassessed. *Earth Science Reviews*, 45, 1–44.

Gibson, I. L., 1967. Preliminary account of the volcanic geology of Fantale, Shoa. *Bulletin of the Geophysical Observatory Addis Ababa*,10, 59-67.

Gouin P., 1979. *Earthquake History of Ethiopia and the Horn of Africa*. International Development Research Center (IDRC), Ottawa.

Gudmundsson, A., 1992. Formation and growth of normal faults at the divergent plate boundary in Iceland. *Terra Nova*, 4, 464-471.

Hamling I., Wright T.J., Calais E., Bennati L., Lewi E., 2010. Stress transfer between thirteen successive dike intrusions in Ethiopia. *Nature Geoscience*, 3, 713-717.

Hayward, N.J., Ebinger, C.J., 1996. Variations in the along-axis segmentation of the Afar Rift system. *Tectonics*, 15, 244-257.

Kidane, T., Courtillot V., Manighetti I., Audin L., Lahitte P., Quidelleur X., Gillot P.Y., Gallet Y., Carlut J., Haile T., 2003. New paleomagnetic and geochronologic results from Ethiopian Afar: block rotations linked to rift overlap and propagation and determination of a ~2 Ma reference pole for stable Africa, *Journal of Geophysical Research, 108,* 2102, doi: 10.1029/2001JB000645.

Johnsen, S. J., Dahl-Jensen, D., Dansgaard, W., Gundestrup, N. 1995. Greenland palaeotemperatures derived from GRIP borehole temperature and ice core profiles. *Tellus* 47B, 624–629.

Lahitte, P., Coulie E., Mercier N., Kidane T., Gillot P.Y., 2001. Chronologie K-Ar et TL du volcanisme aux extremites sud du propagateor mer Rouge en Afar depuis 300 ka, *C.R. Acad. Sci. Paris, Earth and Planetary Sciences, 332,* 13-20.

Lahitte P., Gillot P.Y., Kidane T., Courtilllot V., Abebe, B., 2003. New age constraints on the timing of volcanism in Central Afar, in the presence of propagating rifts, *Journal of Geophysical Research, 108,* 2123, doi: 10.1029/2001JB001689.

Le Pichon X., Francheteau J., 1978. A plate tectonic analysis of the Red Sea-Gulf of Aden area. *Tectonophysics,* 46, 369-406.

Miall A.D.,1985. Architectural-element analysis: a new method of facies analysis applied to fluvial deposits. *Earth Science Review*, 22, 261-308.

Miall A.D., 1996. The Geology of fluvial deposits. *Springer Ed*., 582 pp.

Morton W.H. & Black R., 1975. Afar Depression of Ethiopia. In: Pilger A., Rösler A. (Eds.), Afar Depression of Ethiopia, *Proceedings of an International Symposium on the Afar Region and Related Rift Problems, Bad Bergzabern, F.R. Germany, April 1-6, 1974, vol. 1. E. Schweizerbart'sche Verlagsbuchhandlung*, pp. 55-61.

Manighetti I., Tapponier P., Courtillot V., Gallet Y., Jacques E., Gillot, P.Y., 2001. Strain transfer between disconnected propagation rifts in Afar. *Journal of Geophysical Research,* 106, 13613-13665.

Mengesha Tefera, Tadiwos Chernet & Workineh Haro, 1996. *Explanation of the geological map of Ethiopia*. *Scale 1:2.000.000*. 2nd Edition, Ethiopian Institute of Geological Survey, 80 pp. 2nd ed. EIGS, Addis Ababa.

McKenzie, D.P., Davies, D., Molnar, P., 1970. Plate tectonics of the Red Sea and East Africa. Nature 226, 243-248.

Mohr, P.A., 1962. Surface Cauldron Subsidence with associated faulting fissure basalt eruption at Gariboldi pass, Shoa. Bulletin of Volcanology 24, 421-428.

Mohr P., 1986. *Sequential aspects of the tectonic evolution of Ethiopia*. Mem. Soc. Geol. It. 31, 447–461.

Pizzi A., Pomposo G., Abebe B. & Coltorti M., 2008. - Stile deformativo e reticolo idrografico lungo la scarpata del Plateau Somalo al margine meridionale dell'Afar (Etiopia). Rendiconti online Società Geologica Italiana, 1, 137-139.

Pizzi A. & Pontarelli L., 2007. Geometria del rift nel margine meridionale dell'Afar: Dire Dawa (Etiopia). Rend. Soc. Geol. It., **4**, 288-289

Rampey, M.L., Oppenhaimer C., Pyle D.M., Yirgu G., 2010. Caldera-forming eruptions of the Quaternary Kone Volcanic Complex, Ethiopia. Journal of African Earth Sciences, 58, 51-66.

Rowland, J.V., Baker, E., Ebinger, C.J., Keir, D., Kidane, T., Biggs, J., Hayward, N., Wright, T.J., 2007. Fault growth at a nascent slow-spreading ridge: the 2005 Dabbahu rifting episode, Afar. Geophys. J. Int., 171, 1226-1246.

Salvador, A. 1994. International Stratigraphic Guide. A guide to stratigraphic classification, terminology and procedures. The International Union of Geological Science and the Geological Society of America (Eds), 214 pp.

Sigmundsson, F., 2006. Magma does the splits. Nature, 442, 251-252.

Tapponier P., Armijo R., Manighetti I., Courtillot V., 1990. Bookshelf faulting and horizontal block rotations between overlapping rifts in southern Afar. Geophysical Research Letters, 17, 1-4.

Vanderberghe, J., 2002. The relation between climate and river processes, landforms and deposits during the Quaternary. Quaternary International 91, 17–23.

Wright, T.J., Ebinger, C., Biggs, J., Ayele, A., Yirgu, G., Keir, D., Stork, A., 2006. Magma maintained rift segmentation at continental rupture in the 2005 Afar dyking episode. Nature, doi: 10.1038/nature04978.